TECHNICAL REPORT
NATICK/TR-79/009

ON THE NOTIONS OF FREE DROP AND FRAGILITY RATINGS

by

Franklin Barca

OCTOBER 1978

UNITED STATES ARMY
...and DEVELOPMENT COMMAND
...MASSACHUSETTS 01760

Aero-Mechanical Engineering Laboratory

UNCLASSIFIED

SECURITY CLASSIFICATION OF THIS PAGE (When Data Entered)

(14)

REPORT DOCUMENTATION PAGE

READ INSTRUCTIONS BEFORE COMPLETING FORM

1. REPORT NUMBER: NATICK/TR-79/009	2. GOVT ACCESSION NO.
3. RECIPIENT'S CATALOG NUMBER: (9)	
4. TITLE (and Subtitle): (6) ON THE NOTIONS OF FREE DROP AND FRAGILITY RATINGS.	5. TYPE OF REPORT & PERIOD COVERED: Final rept. Jan 1976–Sept 1978
	6. PERFORMING ORG. REPORT NUMBER
7. AUTHOR(s): (10) Franklin Barca	8. CONTRACT OR GRANT NUMBER(s)
9. PERFORMING ORGANIZATION NAME AND ADDRESS: US Army Natick Research & Development Command, Aero-Mechanical Engineering Laboratory, Natick, Massachusetts 01760	10. PROGRAM ELEMENT, PROJECT, TASK AREA & WORK UNIT NUMBERS: (6) 6.21L162210D283,035BG,048 BG
11. CONTROLLING OFFICE NAME AND ADDRESS: US Army Natick Research & Development Command, Aero-Mechanical Engineering Laboratory, Natick, Massachusetts 01760 (11)	12. REPORT DATE: October 1978 (13) 03 13. NUMBER OF PAGES: 62
14. MONITORING AGENCY NAME & ADDRESS (if different from Controlling Office): (12) 64p.	15. SECURITY CLASS. (of this report): UNCLASSIFIED 15a. DECLASSIFICATION/DOWNGRADING SCHEDULE

16. DISTRIBUTION STATEMENT (of this Report)

Approved for public release, distribution unlimited

17. DISTRIBUTION STATEMENT (of the abstract entered in Block 20, if different from Report)

18. SUPPLEMENTARY NOTES

19. KEY WORDS (Continue on reverse side if necessary and identify by block number)

AERIAL DELIVERY	PACKAGING
AIRDROP OPERATIONS	FRAGILITY
FREE FALL	ENERGY ABSORBERS
IMPACT	DISSIPATION

20. ABSTRACT (Continue on reverse side if necessary and identify by block number)

Free drop is the air-to-ground delivery of supplies and equipment without the aid of conventional recovery parachutes. This study was conducted to determine the present state of the art in free drop aerial delivery and to identify areas which require additional investigation to expand the military free drop capability. Results of the study indicate that future effort would be best expended in the areas of fragility rating determination and improved packaging methods for subsistence items such as food, clothing, and water. A bibliography is also included.

DD FORM 1 JAN 73 1473 EDITION OF 1 NOV 65 IS OBSOLETE

392674

UNCLASSIFIED

SECURITY CLASSIFICATION OF THIS PAGE (When Data Entered)

TABLE OF CONTENTS

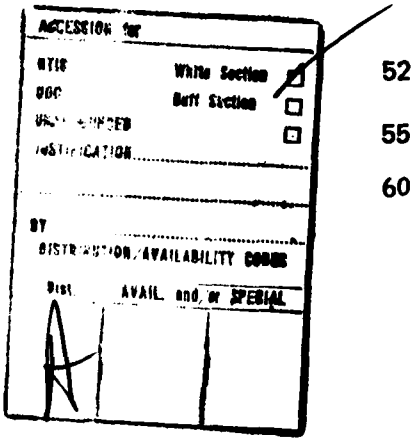

LIST OF FIGURES

LIST OF FIGURES (Continued)

ON THE NOTIONS OF FREE DROP AND FRAGILITY RATINGS

INTRODUCTION

Free drop is the air-to-ground delivery of supplies or equipment without the aid of conventional recovery parachutes. Of all the various types of aerial delivery possible; for example, parachutes, gliding decelerators and retro rockets, free drop is the simplest and least expensive because it does not require a decelerator and the associated rigging. It can also be very accurate because the payload traverses the airspace rapidly and is not, therefore, subject to as much wind drift error as a parachute-retarded airdrop.

All items, certainly, cannot be successfully free-dropped; many are too fragile and would be destroyed upon impact. A large number of small rugged items such as clothing, rations, potable water and possibly ammunition do exist, however, which show potential for successful free drop. In fact, systems have been developed in the past by both Governmental and private agencies which have successfully free-dropped a variety of items such as food, clothing, electronic sensors and transmitting equipment to remote generally inaccessible areas.

A critical parameter in determining which items may be free-dropped without damage is the "fragility rating" of the item. The fragility rating is a measure of the inherent ruggedness of the item. The larger the fragility rating the stronger the item is and the better are its chances of survival upon impact. Fragility ratings have been determined for much electronic gear but generally have not been developed for common military resupply items.

Free drop, then, has the potential to be a simple, inexpensive, and accurate alternative method of aerial delivery and has been used successfully to deliver certain specific payloads. Because of these reasons and because the Army has conducted only limited research in this area in the recent past this study was initiated. The objective of the study was to:

Determine the present state of the art in free-drop aerial delivery.

Identify critical parameters which must be addressed to design a free-drop system.

Identify areas which require additional investigation to improve and expand military free-drop capability.

The study is divided into three parts: Free fall dynamics and aerodynamics, impact dynamics and fragility, and shock mitigating methods and packaging. A bibliography is also included.

FREE FALL DYNAMICS AND AERODYNAMICS

Many variables affect the dynamics and aerodynamics of a freely falling body. The problem is to determine the relationship between the variables as they exist in a free drop aerial delivery situation. The primary goal is to develop the ability to analytically predict the payload impact point, impact velocity, and orientation and to mathematically model that portion of the delivery cycle between aircraft ejection and ground impact. The effect of the variables on the trajectory and consequently impact point accuracy can then be predicted, computer simulated and promising schemes experimentally verified.

State of the Art

Much work has been accomplished in this area. The aerodynamic factors have been identified and many basic relationships have been developed.

Streeter and Olson[1] presented a derviation of the equations of motion of a freely falling body and compared a step-wise calculation and a graphical integration method of determining a container trajectory. Semigraphical methods[2,3] have been developed to predict the motion of both the container and parachute during retarded airdrop. Turnacliff and Hartnett[4] presented a trajectory analysis solution in series form for determination of the velocity history of a parachute as a function of the "weight-to-drag" ratio, initial altitude, and initial velocity.

Following these methods, the equation of motion for a free-falling body in a uniform gravitational field may be established and solved assuming an isothermal atmosphere, constant drag coefficient, negligible lift compared to drag, and zero wind condition. Referring to Figure 1 and defining the following symbols, the equations of motion are derived:

[1] Streeter, V. L. Determination of Momentum of Air Dropped Shipping Containers. (Two ITT reports), November 1949 (AD 473134); March 1950 (AD 473135)

[2] Design for Air Transport and Airdrop of Material – Engineering Design Handbook. AMCP 706–130, December 1967.

[3] Low Altitude Air Drop System. ER 3980. Aircraft Armaments, Inc., May 1965.

[4] Turnacliff and Hartnett. Generalized Trajectories for Free-Falling Bodies of High Drag. WADC, August 1957. (AD 142300)

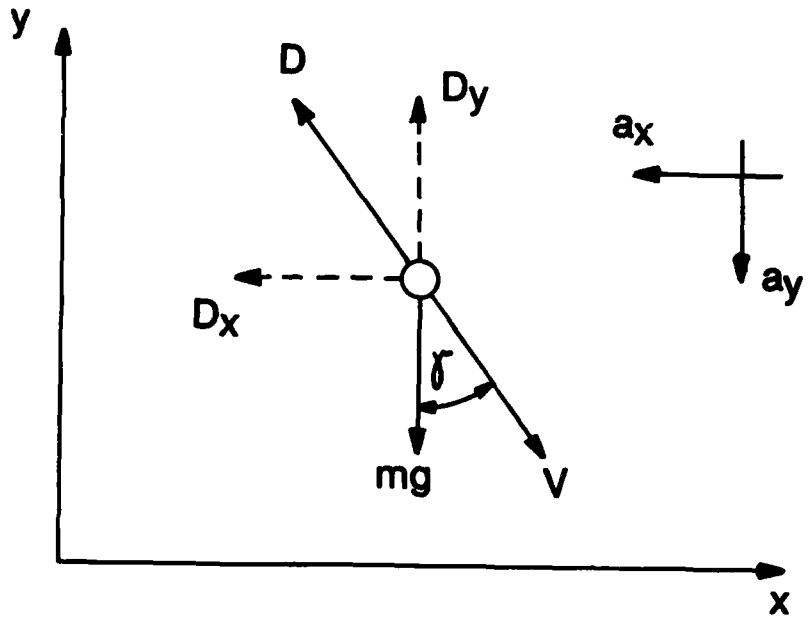

Figure 1. Free Falling Body Diagram. Sign Convention and Vector Identification

a	Payload acceleration	m/s^2
a_x	Horizontal components of payload acceleration	m/s^2
a_y	Vertical component of payload acceleration	m/s^2
C_D	Payload drag coefficient	--
D	Drag force on payload	N
D_x	Horizontal component of drag force	N
D_y	Vertical component of drag force	N
F_x	Horizontal component of force	N
F_y	Vertical component of force	N
g	Acceleration due to gravity	m/s^2
K	Resistance parameter	s^2/m^2

M	Payload mass	kg
S	Projected payload area	m^2
V	Payload velocity	m/s
V_T	Terminal velocity	m/s
V_x	Horizontal component of payload velocity	m/s
V_y	Vertical component of payload velocity	m/s
V_{y_1}	Former vertical velocity component	m/s
V_{y_2}	New vertical velocity component	m/s
V_x	Average payload velocity in horizontal direction	m/s
V_y	Average payload velocity in vertical direction	m/s
X_1	Former horizontal coordinate	m
X_2	New horizontal coordinate	m
Y_1	Former vertical coordinate	m
Y_2	New vertical coordinate	m
γ	Angle between velocity vector and vertical component	(deg)
ρ	Density of air	kg/m^3
Δt	Time increment	s
ΔV_x	Change in payload horizontal velocity	m/s
ΔV_y	Change in payload vertical velocity	m/s
ΔX	Incremental payload displacement in horizontal direction	m
ΔY	Incremental payload displacement in vertical direction	m

Summing the forces in the Y direction,

$$\Sigma F_y = ma_y$$

$$-mg + D_y = -ma_y$$

assuming $D = \frac{1}{2}\rho C_D S V^2$

then $D_y = \frac{1}{2}\rho C_D S V^2 \cos\gamma$

and $$-mg + \frac{1}{2}\rho C_D S V^2 \cos\gamma = -ma_y \qquad (1)$$

but $\cos\gamma = V_y/V,$

$$-mg + \frac{1}{2}\rho C_D S V V_y = -ma_y$$

$$a_y = g - \left(\frac{\rho C_D S}{2m}\right) V V_y$$

and the change in the vertical velocity component due to acceleration over the time interval Δt is

$$\Delta V_y = a_y \Delta t$$

and the vertical velocity after the time interval Δt is

$$V_{y_2} = V_{y_1} + \Delta V_y \qquad (2)$$

and the change in vertical position over the time interval Δt is

$$\Delta Y = \frac{V_{y_1} + V_{y_2}}{2} \Delta t$$

and the new vertical position after the time interval Δt is

$$Y_2 = Y_1 + \Delta Y \qquad (3)$$

Similarly summing the forces in the horizontal direction

$$\Sigma F_x = ma_x$$

$$-D_x = -ma_x$$

$$a_x = \frac{D_x}{m}$$

$$a_x = \frac{1}{m}\left(\frac{1}{2}\rho C_D S\right)\left(V^2 \sin\gamma\right)$$

where

$$\sin\gamma = V_x/V, \quad \therefore$$

$$a_x = \frac{\rho C_D S}{2m} VV_x$$

or

$$a_x = g\ KVV_x \tag{4}$$

where $K = \frac{\rho C_D S}{2mg}$ and is defined as the resistance parameter and

$$V_{x_2} = V_{x_1} + \Delta V_x \tag{5}$$

and

$$x_2 = x_1 + \Delta X \tag{6}$$

In addition, when the horizontal velocity component has decreased to zero as a result of air friction, and the drag force in the vertical direction is equal to the gravitational force, the vertical acceleration also decreases to zero and a condition of constant or terminal velocity is attained. From equation (1):

$$g = \left(\frac{\rho C_D S}{2m} \right) VV_y$$

and $V = V_y = V_T$ where V_T is the terminal velocity

$$V_T^2 = \frac{2gm}{\rho C_D S}$$

or

$$V_T = \sqrt{\frac{2gm}{\rho C_D S}}$$

or

$$V_T = \sqrt{1/K} \tag{7}$$

Equations (1) through (7) define the theoretical trajectory of a body in free fall. The major variables which affect the theoretical trajectory are:

Initial position

Initial velocity

Payload mass

Payload surface area

Drag coefficient

Air density

Gravitational acceleration

Wind speed and direction

Effect of Initial Position

Any error between the computed air release point and the actual aircraft position and heading at the time of release will cause an error between actual and calculated impact point. Initial position errors can be caused by navigational errors, the location of the load in the aircraft, and the method of load ejection or extraction. For the purposes of this study it is assumed that the position of the payload upon release is accurately known in relation to the calculated impact point.

Effect of Initial Velocity

The initial velocity of the cargo at release is the same as the aircraft velocity relative to the ground. Figure 2 illustrates the effect of various initial horizontal velocity

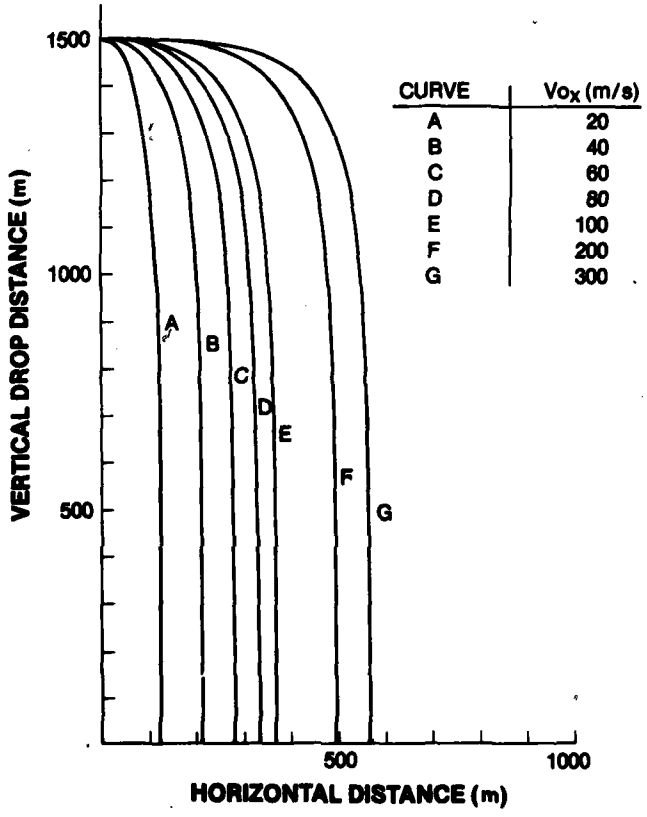

Figure 2. Flight Path of Freely Falling Object with K = 5 x 10^{-4} s^2/m^2 for Various Horizontal Velocities

components on the trajectory of a freely falling object with a resistance parameter, K=0.0005 s^2/m^2, and a zero initial vertical velocity component. Although the resistance parameter is used as an index in the figure, the terminal velocity could also be used as an equivalent index because the two are related as shown in equation (7). The standard sea level density relationship between the terminal velocity and resistance parameters cited in the following figures is shown in Table 1.

Table 1. Relationship between resistance parameter and terminal velocity at standard sea level conditions.

RESISTANCE PARAMETER K (s^2/m^2)	TERMINAL VELOCITY V_T (m/s)
1×10^{-2}	10.0
5×10^{-3}	14.1
5×10^{-4}	44.7
4×10^{-4}	50.0
1.5×10^{-4}	81.6
1×10^{-4}	100.0
5×10^{-5}	141.4

If the aircraft is in a steady climb or dive at the instant the cargo is released, the cargo has an equivalent vertical velocity component also. The trajectories which result when the same object is released from an aircraft with a horizontal velocity component of 100 m/s and various initial vertical velocity components are plotted in Figure 3. As

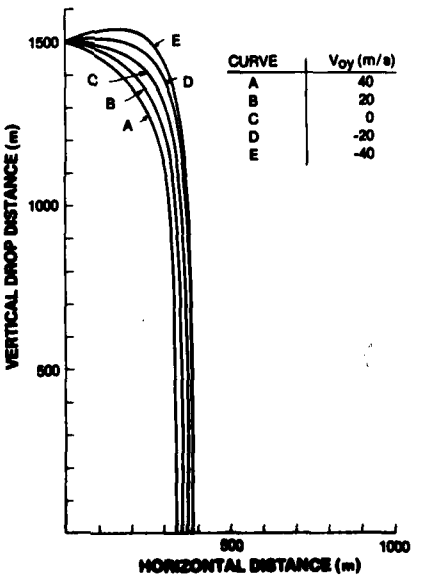

Figure 3. Flight Path of Freely Falling Body with $K = 5 \times 10^{-4}$ s^2/m^2 and $V_{ox} = 100$ m/s for Various Initial Vertical Velocities

expected, the horizontal velocity component has a greater effect than the vertical velocity component on the forward travel distance of the payload.

After release the horizontal velocity decreases due to air resistance while the vertical velocity increases, normally to a limit, due to gravitational attraction. Figures 4 through 7 illustrate the changes in horizontal and vertical velocity components for a freely falling body with various initial velocities and resistance parameters. As previously mentioned changes in air density, drag coefficient, drag area and payload mass all cause changes in the resistance parameter.

Figures 8 through 11 are total velocity profiles for freely falling objects with various resistance parameters. It is interesting to note in these figures that for some cases the velocity of the falling body initially decreases and then increases. This indicates that there exists an optimum drop altitude for minimizing impact velocity and consequently payload kinetic energy. Also, as shown in Figure 10, containers with a resistance parameter

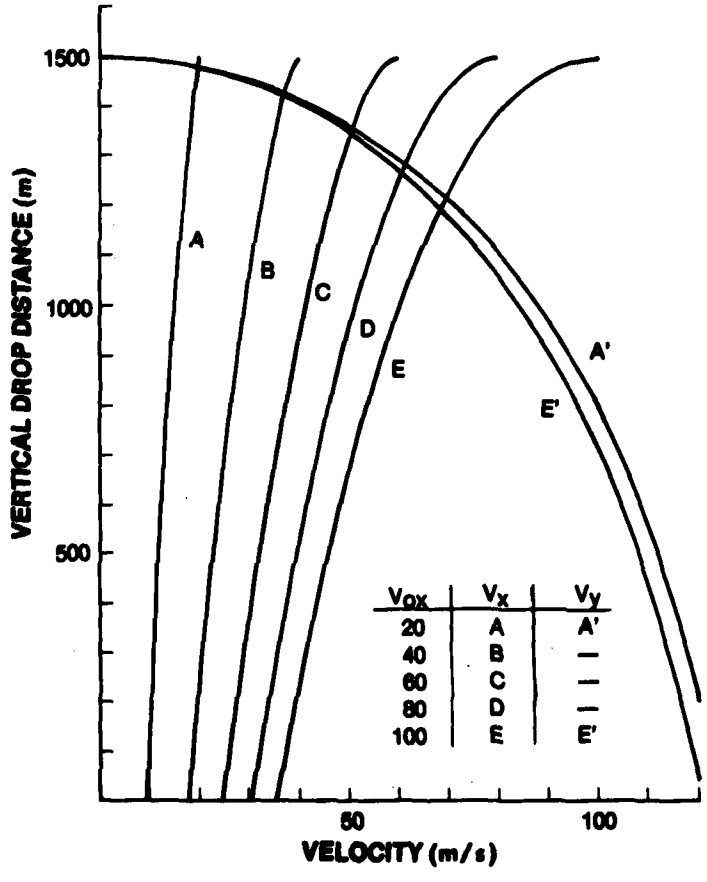

Figure 4. Change of Velocity Components for Freely Falling Body with $K = 5 \times 10^{-5}$ s^2/m^2

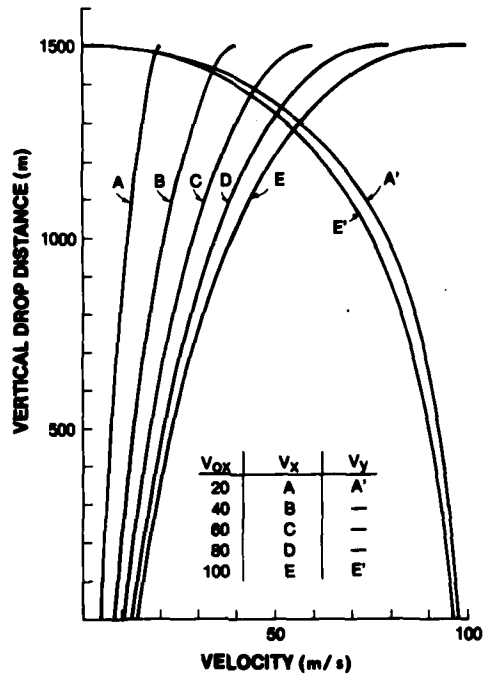

Figure 5. Change of Velocity Components for Freely Falling Body with $K = 10^{-4}\ s^2/m^2$

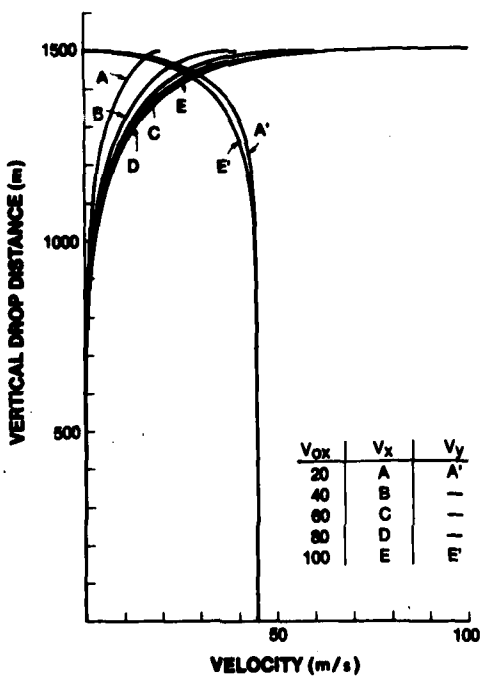

Figure 6. Change of Velocity Components for Freely Falling Body with $K = 5 \times 10^{-4}\ s^2/m^2$

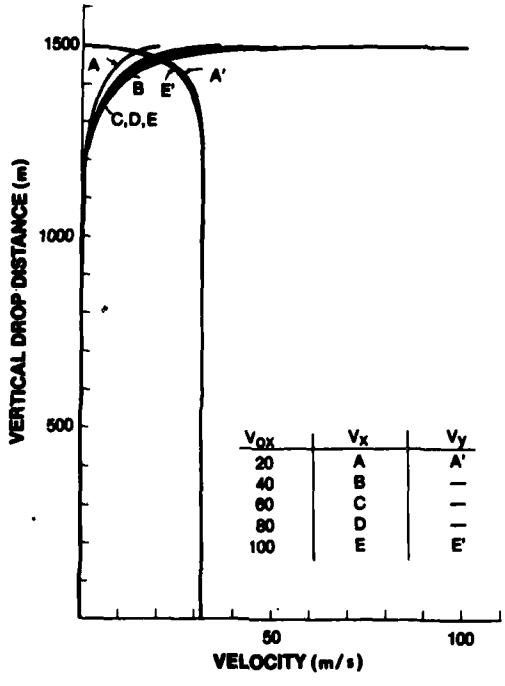

Figure 7. **Change of Velocity Components for Freely Falling Body with $K = 10^{-3}\ s^2/m^2$**

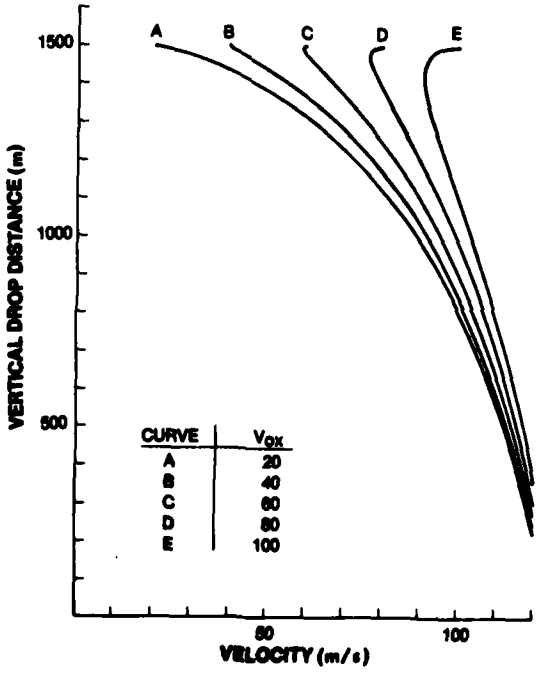

Figure 8. **Velocity of Freely Falling Body with $K = 5 \times 10^{-5}\ s^2/m^2$**

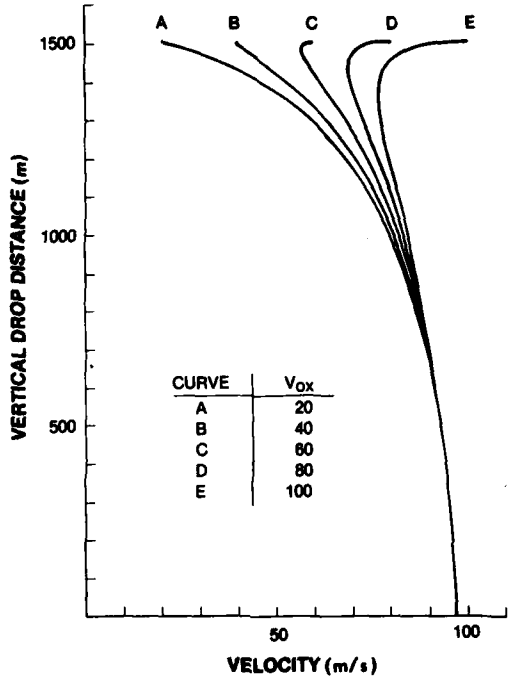

Figure 9. Velocity of Freely Falling Body with K = 10^{-4} s^2/m^2

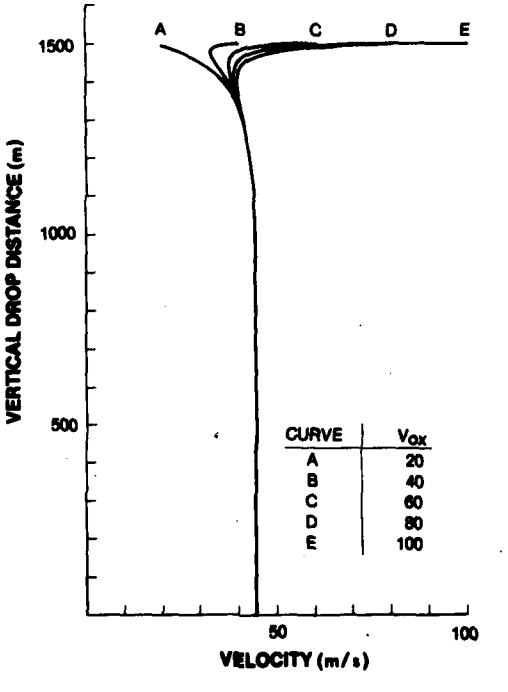

Figure 10. Velocity of Freely Falling Body with K = 5 x 10^{-4} s^2/m^2

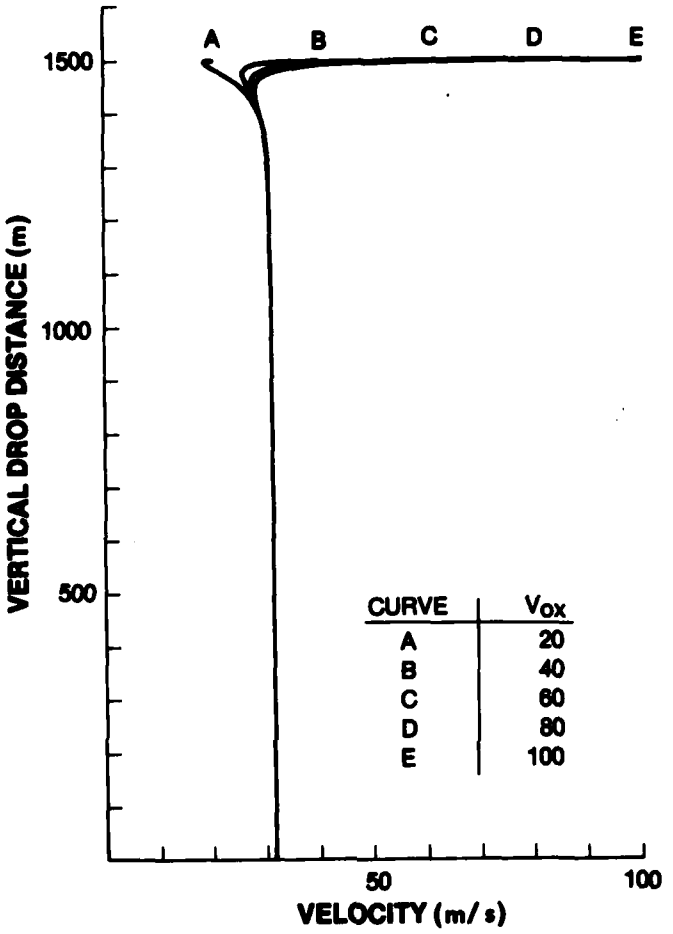

Figure 11. Velocity of Freely Falling Body with K = 10^{-3} s^2/m^2

of 0.0005 s^2/m^2 or greater may be dropped at a wide range of initial velocities with minimum effect on the resulting velocity and consequently impact momentum after a 200-metre fall. Considering representative resupply items and regardless of initial horizontal velocity, an A–22 container load of four 208-litre (55 gallon) water-filled drums, Figure 12, attains a terminal velocity of approximately 80 metres/sec after a free drop of 1,000 metres and a container of combat rations, Figure 13, attains a terminal velocity of 50 metres/sec after a 500-metre free drop.

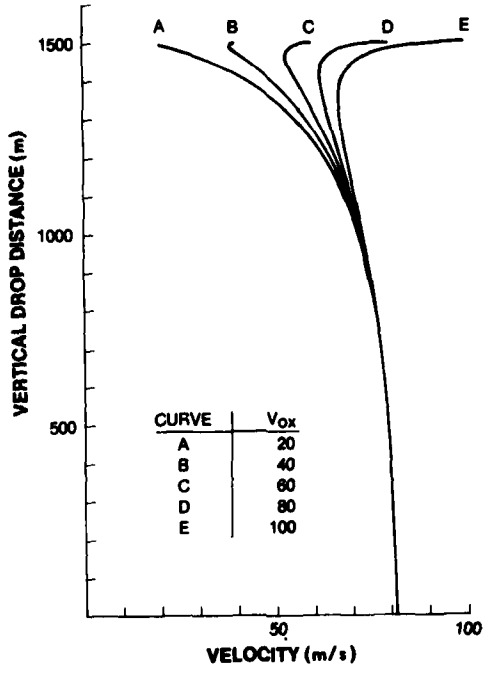

Figure 12. Velocity of Freely Falling A–22 Container with K = 1.5 x 10^{-4} s^2/m^2

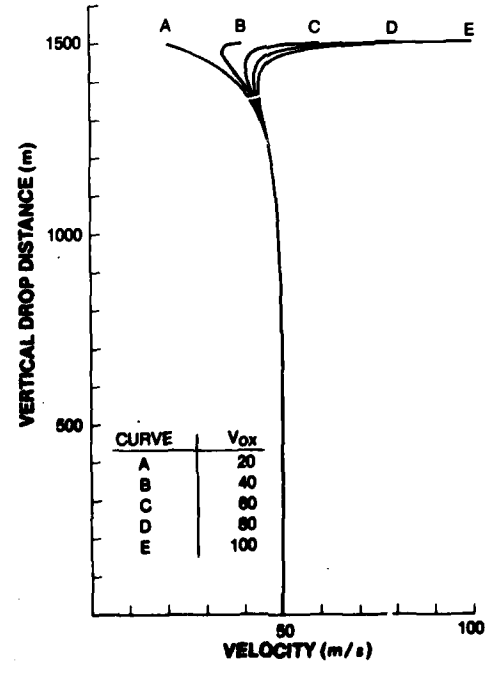

Figure 13. Velocity of Freely Falling Ration Container with K = 4 x 10^{-4} s^2/m^2

It has been assumed that aircraft characteristics do not affect the payload trajectory. However, one result of a free fall delivery study conducted by Dehmer[5] indicated that a given load would not follow the same trajectory, when free dropped under the same conditions, from two different types of aircraft. In a series of drops of 800-kilogram A–22 containers, the horizontal distance and time of fall from a C–119 aircraft was found to be consistently shorter than that published for the C–130 aircraft. No definite explanation of the anomaly was found and different ballistics data, Figure 14, were published[6] for identical loads dropped under identical conditions from two different types of aircraft. The anomaly may be the result of characteristics associated with the aircrafts.

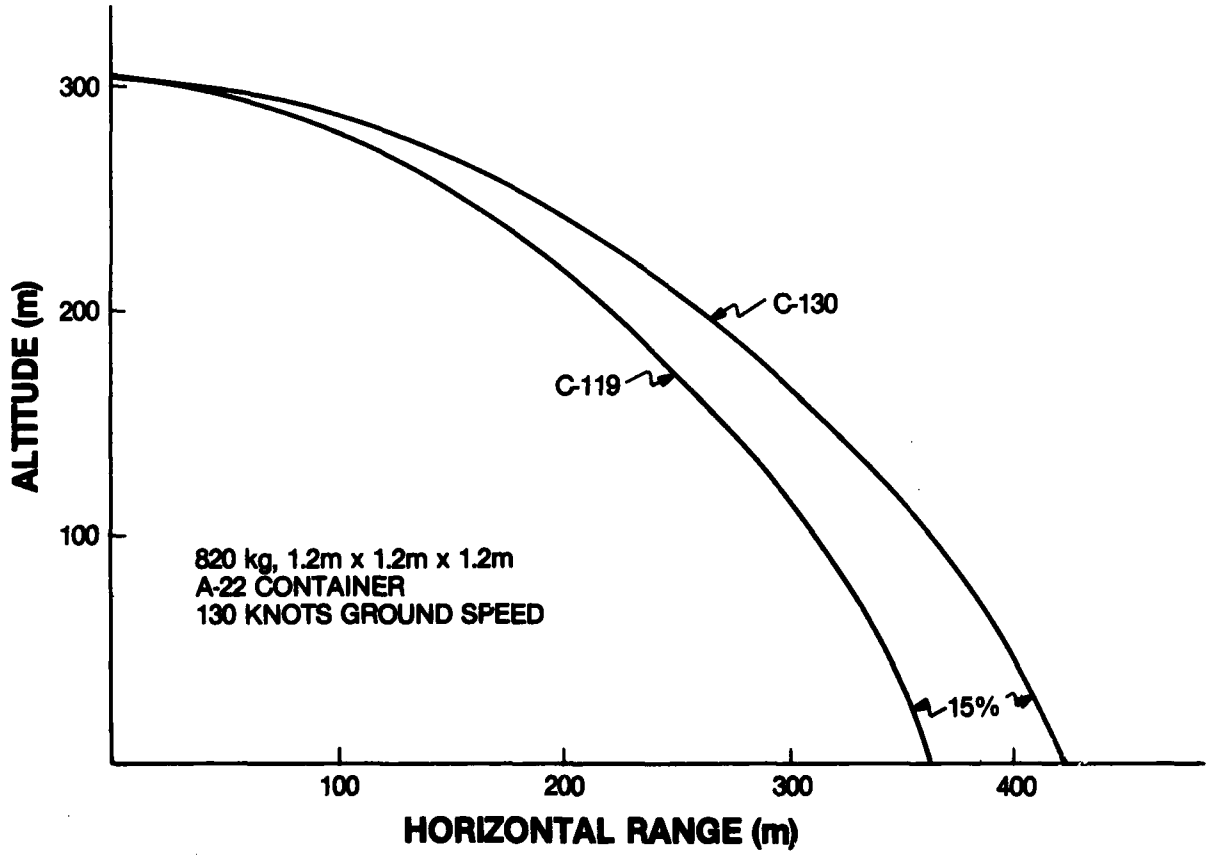

Figure 14. C119 and C130 Ballistics Data

[5]Dehmer, P. A. Free Fall Delivery, C–119 Aircraft. TAC Test 68–208, June 1969. (AD 864073)

[6]Computed Air Release Systems Procedures. TACM 55–40 November 1971.

Effect of Payload Mass, Projected Area and Drag Coefficient

The payload mass, projected area and drag coefficient all affect the velocity, horizontal travel distance and time of flight of a freely falling object. Other factors held constant: the velocity (Figure 15) and horizontal travel distance (Figure 16) increase with an increase in mass or decrease in area or decrease in drag coefficient; and the time of flight (Figure 17) increases with an increase in area or increase in drag coefficient or decrease in mass.

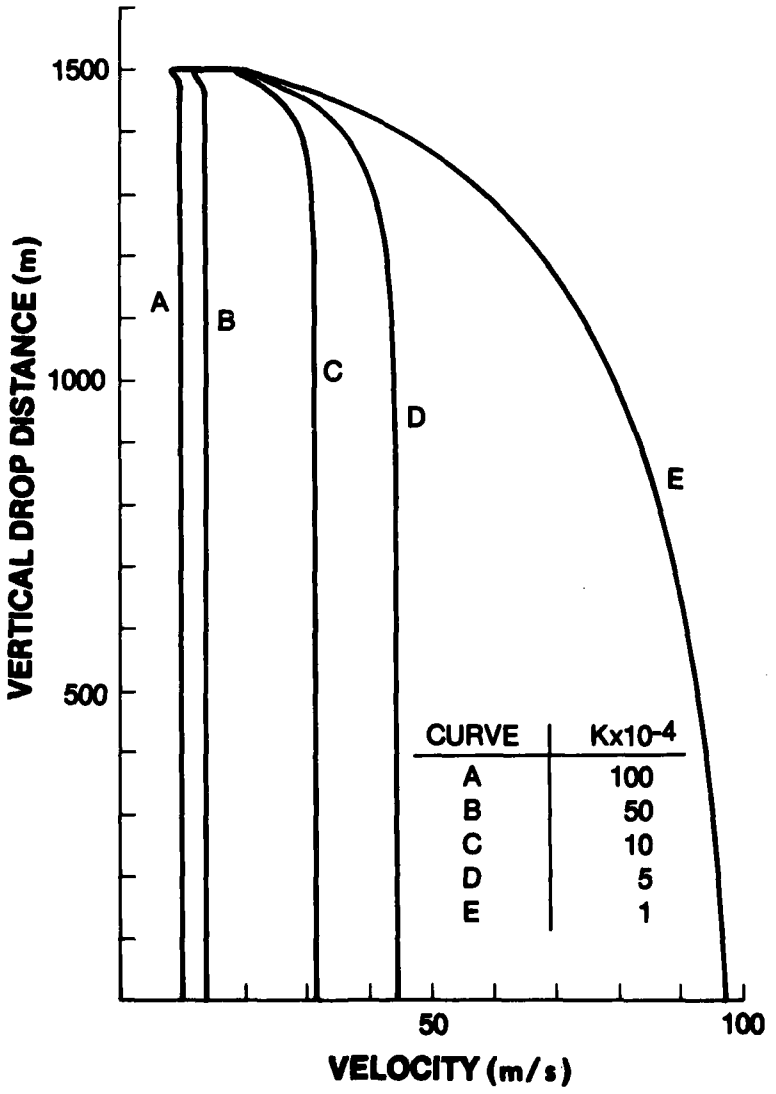

Figure 15. Velocity of Freely Falling Body with V_{ox} = 20 m/s for Various Resistance Parameters

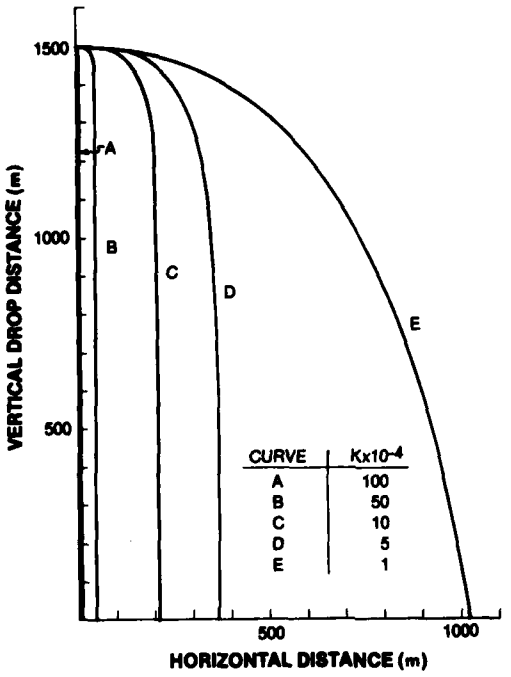

Figure 16. **Flight Path of Freely Falling Object with V_{ox} = 100 m/s for Various Resistance Parameters**

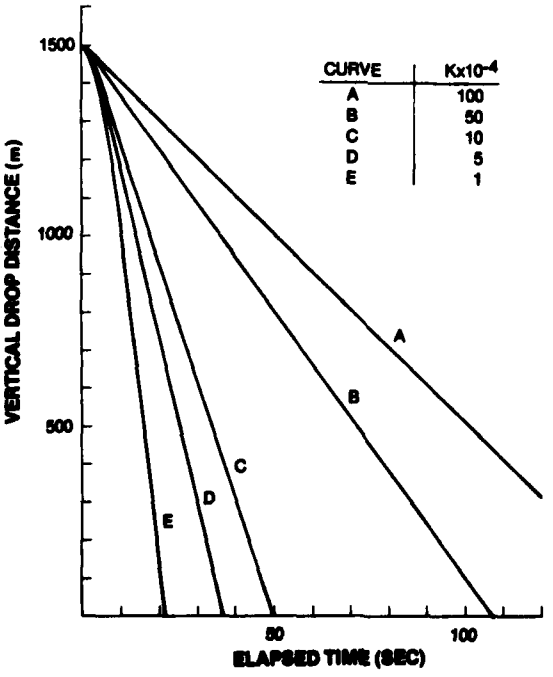

Figure 17. **Drop Time for Freely Falling Body with V_{ox} = 20 m/s for Various Resistance Parameters**

The trajectory equations assume experimentally verified constant drag coefficients and a constant payload projected area. In reality these assumptions are not valid.

Although Hoerner[7] has compiled a useful collection of practical drag data; such as for plates, rectangles and rotating cubes, drag coefficients are still unavailable for many items and have only recently been published[8] for the basic A–22 aerial delivery container.

In addition, during free fall, a payload could be randomly tumbling and the drag coefficients and projected area would be constantly changing. For example, in a free drop test of Thai combat rations[9], no correlation could be made between impact velocity and system mass for similar shaped items free dropped under identical conditions from the same helicopter. If not experimental error, this could be the result of changes in projected area and drag coefficients as a result of tumbling during free fall.

Attempts[8,10-13] to stabilize a payload by streamlining, addition of fins, and/or proper positioning of the center of gravity/pressure have been made with various degrees of success. In addition to preventing tumbling, payload stabilization results in impact upon a predetermined payload surface. Some items have a greater fragility rating, i.e., are more rugged, in one axis than the other. Ideally that is the axis which should be subjected to impact for maximum possibility of survival. Also, if the impact surface is known, only that surface need be protected with an energy absorber. If the impact surface is unknown, the entire payload surface may require some type of cushioning.

[7] Hoerner, S. F. Fluid Dynamic Drag. Hoerner Fluid Dynamics. 1965

[8] Barnard, G. *et. al.* Development of a High Level Container Airdrop System. AIAA Paper No. 75–1386, November 1975.

[9] Ilves and Fiorentio. Free Drop Test of Thai Combat Ration. July 1967. (AD 822885)

[10] Development of 25-Gallon Free Drop Aerial Delivery Fuel Containers. US Rubber Co., December 1958.

[11] Heick, R. J. Dynamic Energy Absorbing Characteristics of Paper Honeycomb Determined by Airdrops. (Five QMFCIAF reports): No. 70, April 1955 (AD 73431); No. 74, May 1955 (AD 73432); No. 98, October 1955; No. 99, October 1955; No. 108, December 1955.

[12] Venetos, M. A. Design of Load Configurations for the M–4 High Speed Aerial Delivery Container. (Eight QMFCIAF reports); No. 14–59, May 1959; No. 22–59, June 1959; No. 203, July 1959; No. 28–59, October 1959; No. 3–60, February 1960; No. 217, June 1960; No. 19–60, July 1960; No. 4–61, March 1961.

[13] Williams, E. F. Research on Experimental High Velocity Airdrop Systems. QMFCIAF No. 170, February 1956.

Numerous studies[14-18] have investigated means other than conventional parachutes such as rotors, aerodynamically shaped containers, and toroids to decelerate a payload during free drop. Generally these systems are designed for expensive payloads and are not applicable to common resupply items.

A simple system to decelerate resupply items during free drop has been suggested[9,19] but not fully tested. In this system a pallet load of ration containers is dropped from an aircraft as a single unitized load. Sometime shortly before impact the straps holding the load together are cut and the individual containers disperse. Because the resistance parameter of the individual containers is greater[11] than that of the unitized load, the individual containers experience a decrease in velocity as shown in Figure 18. The individual containers impact with approximately 63% of the velocity that the unitized load would have impacted with. Considering equal masses, this means that the total kinetic energy of the ration containers at impact is only 40% as great as the unitized load.

[14] Investigation of Stored Energy Rotors for Recovery. WPAFB ASD–TDR–63–745, December 1963.

[15] Container, Free Drop, Map and Photo. Republic Aviation Corp., September 1960.

[16] McCollough, R. B. The Construction of a Toroidal Deceleration/Flotation Device. AFSWC–TR–73–44, December 1973 (AD 915754L)

[17] Penn, J. Feasibility Study of Rotochute Decelerator for Tactical Weather Buoy. Naval Avionics Facility TR–1015, April 1976 (AD 891605L)

[18] White, G. B. A Design Analysis of Directional Control Systems Applicable to Air Dropped Packaging. Midwest Research Inst. Report, February 1956.

[19] Burt, T. E. Engineer Design Test of Meal, Ready to Eat, Individual. May 1964 (AD 857785)

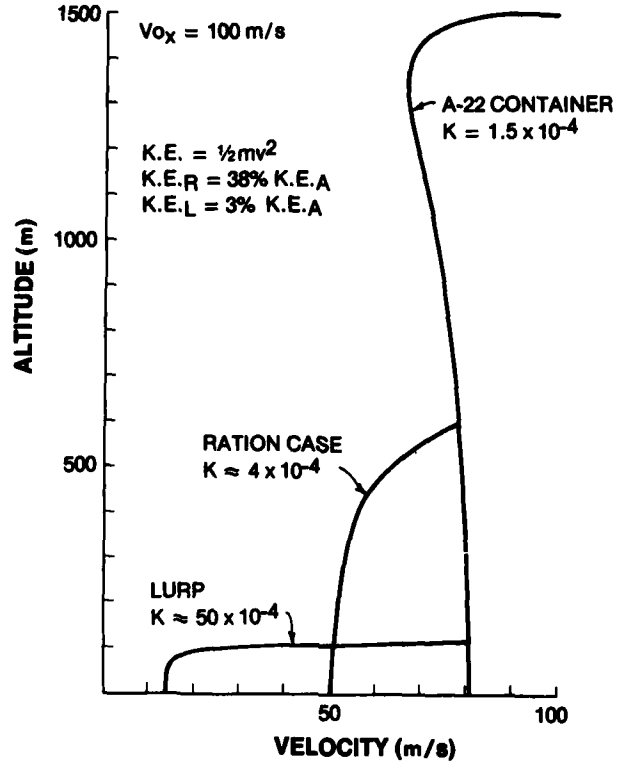

Figure 18. Effect of Mid-Air Dispersion on Impact Velocity

Effect of Air Density

Air density is a function of altitude and temperature. From the Earth's surface to a height of 8 to 16 kilometres, depending on location, the lapse rate, i.e., the rate of decrease of temperature with altitude, is almost constant at 6.5°C per kilometre. Utilizing the constant lapse rate and following the method of Dommasch[20] the density may be expressed as:

$$\rho = \rho_1 \left(1 - \frac{H}{85.5T_1} \right)^{4.256}$$

where

ρ = Density (kg/m³) at altitude H

[20] Dommasch, *et.al.* Airplane Aerodynamics. Third Edition. Pitman Aeronautical Publications, 1961.

ρ_1 = Density (kg/m^3) at base of layer, normally 1.225 kg/m^3 at standard conditions

H = Altitude (m)

T_1 = Temperature (°R) at base of layer, normally 518.69°R at standard conditions

Assuming standard conditions, Figure 19 shows that the density at three kilometres is 75% of that at sea level and the altitude/density variations, therefore, must be considered in trajectory calculations for high altitude drops.

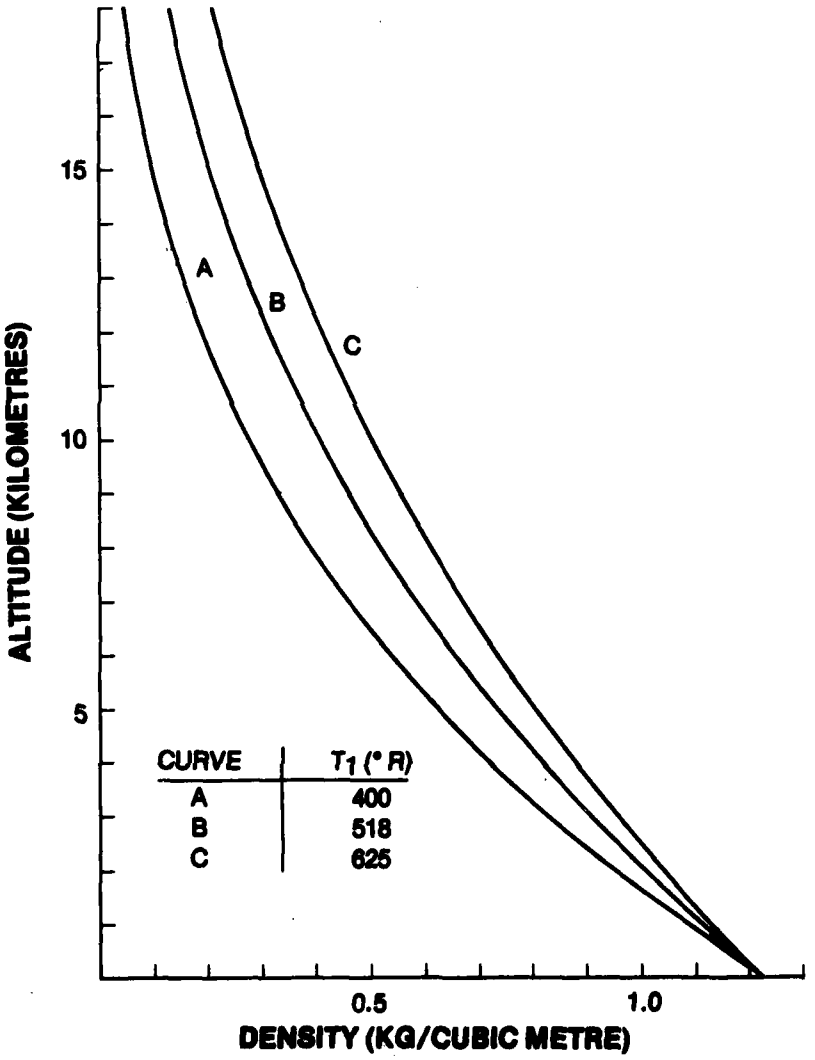

Figure 19. Variation of Atmospheric Density with Altitude and Base Temperature

Effect of Variation in Gravitational Acceleration

Gravitational Acceleration varies with altitude according to the inverse square law:

$$g = g_o \left(\frac{R_o}{R_o + H} \right)^2$$

where,

g = Acceleration of gravity (m/s^2) at altitude H

g_o = Acceleration of gravity (m/s^2) at sea level

R_o = Radius of Earth, assume 6.37×10^6 metres

H = Altitude (m)

But the variation is only one percent below 30 kilometres and can therefore be neglected for practical purposes.

Effect of Wind

Wind speed and direction are uncontrollable variables which may change several times during a descent. Figure 20 illustrates the drift error introduced by winds of various speeds. The error increases with both time of fall and wind speed and can become very significant, especially in parachute-retarded airdrop systems. Petry[21] indicates that the inability to accurately predict wind velocity results in the largest contribution to the overall airdrop error. Farinacci and Bruner[22] compiled a catalog of various representative wind profiles and considered their effects in a computer simulation of a high level container airdrop system. Although wind drift error must be accounted for, it is less severe in free drop than in retarded drop situations because the free drop load traverses the air space more rapidly.

[21] Petry, G. A. Airdrop Error Analysis. WPAFB, June 1975 (ADA 020282)

[22] Farinacci and Bruner. High Level Container Airdrop System. NARADCOM 73–55–AD, March 1973.

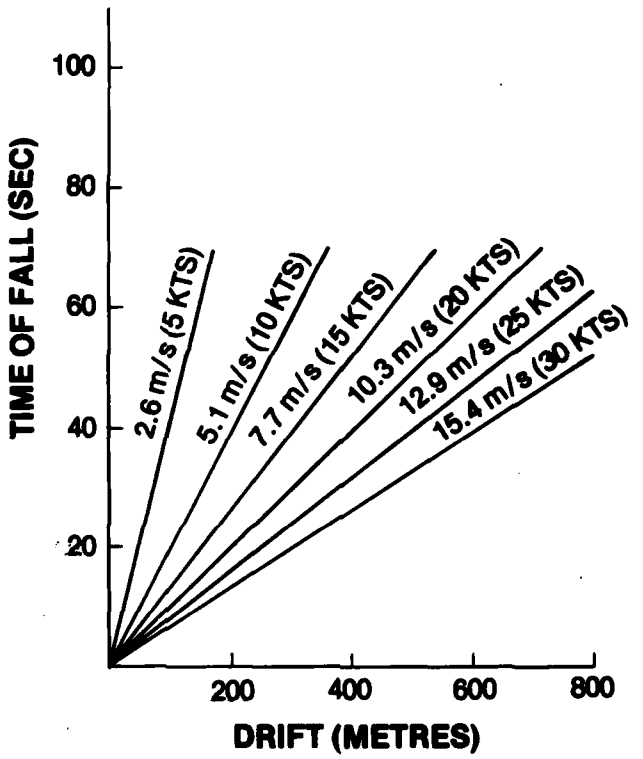

Figure 20. Wind Drift Error

Directions for Future Research

The present state of the art as determined by a literature search is summarized in Table 2. From the table and previous discussion it is concluded that:

(1) The trajectory of a freely falling body can be adequately defined analytically.

(2) A greater knowledge of the individual characteristics of delivery aircraft may decrease trajectory prediction error by as much as 10%.

(3) Sufficient experimental data on drag coefficients of common resupply items are not available. Accurate experimental data would improve theoretical predictions.

(4) Wind drift can be a major source of trajectory error. However, research is being conducted on improved methods to both accurately sense wind speed and direction and to statistically model it. No additional effort is warranted for free drop applications.

(5) Containers which provide both stabilization and deceleration during free drop can be developed and should be considered for non-fragile items.

(6) Individual resupply containers generally acquire less kinetic energy during free drop than unitized loads. Methods of free dropping individual containers which do not substantially increase drop time or scatter are worthy of investigation.

TABLE 2

FREE FALL DYNAMICS & AERODYNAMICS

GOAL: Ability to analytically predict the payload impact point, impact velocity, and orientation.

ANALYSIS:

VARIABLE	STATE OF THE ART				
	Is Effect Definable?	Has it Been Defined?	Experiment Verified?	Sufficient Data Avail?	Can it Be Controlled?
Initial Velocity	Yes	Yes	Yes	Yes	Yes
Initial Position	Yes	Yes	Yes	Yes	Yes
Payload Mass	Yes	Yes	Yes	Yes	Yes
Payload Area	Yes	Yes	Yes	Yes	Yes
Drag Coef.	Yes	Yes	Yes	No	Yes
Air Density	Yes	Yes	Yes	Yes	Yes
Wind Velocity	Yes	Yes	Yes	Yes	No
Wind Direction	Yes	Yes	Yes	Yes	No
Gravitational Var.	Yes	Yes	Yes	Yes	No
Cent. of Grav.	Yes	Yes	Yes	Yes	Yes

DIRECTIONS FOR FUTURE STUDY: Compile existing analytical data and tailor to free drop. Develop needed experimental data.

SIGNIFICANCE OF POSSIBLE RESULTS: Mathematical model required for computer simulation. Experimental data for increased accuracy.

IMPACT DYNAMICS AND FRAGILITY

Upon impact the payload sustains a possibly damaging deceleration shock due to the velocity, attitude and energy developed during free-fall. The problem is to develop an understanding of the damage-producing mechanism of the shock and an understanding of the ability of the payload to withstand the shock without damage. The goal is to develop the ability to analytically predict and experimentally verify the value of the maximum acceleration, the form of the acceleration-time relationship, and the effect of the acceleration on the payload during impact.

State of the Art

Impact Dynamics: An appropriate model of the payload must be chosen to analyze the impact situation. A simple one-degree-of-freedom system will be used initially to illustrate the variables involved. Considering the system of Figure 21, without bottoming or rebound, Mindlin[23] has shown that

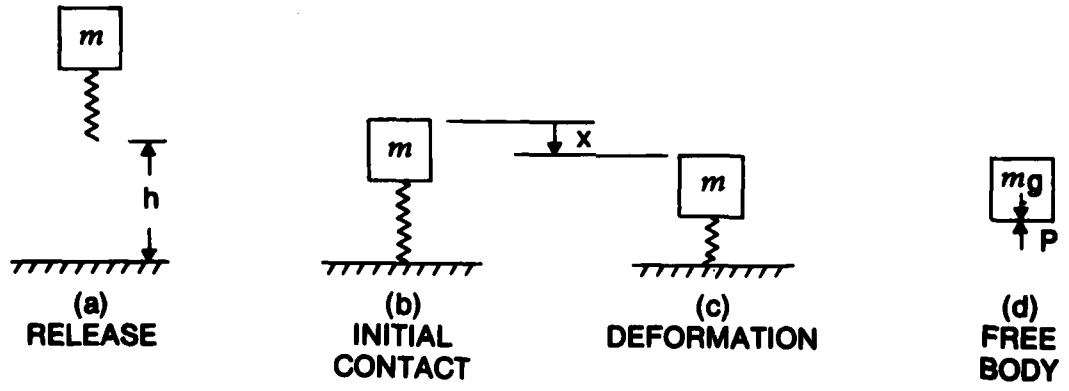

m = ITEM MASS
h = DROP HEIGHT
x = DEFORMATION DISPLACEMENT
P = RESTORING FORCE

Figure 21. Elementary System

[23] Mindlin, R. D. Dynamics of Package Cushioning. Bell Telephone Systems Technical Publications Monograph B–1369, 1945.

$$m\ddot{x} = mg - P$$

and

$$\tfrac{1}{2}m\dot{x}^2 + \int_0^x P\,dx = mg(h + x)$$

where

$\tfrac{1}{2}m\dot{x}^2$ is the instantaneous kinetic energy of m, $\int_0^x P\,dx$ is the energy stored in the spring at any instant, and $mg(h + x)$ is the potential energy of the mass at the initial height $(h + x)$ above the instantaneous position x. Continuing, x is maximum when $\dot{x}$ is zero, therefore,

$$\int_0^{d_m} P\,dx = W\,(h + x)$$

where,

W = weight of item (mg), and

d_m = maximum displacement of the item

For the case of linear elasticity, $P = kx$, where k is the constant spring rate.

Assuming x is significant in comparison to h, (normal airdrop engineering assumption)

$$d_m = \frac{W \pm \sqrt{W^2 + 2Whk}}{k}$$

Or assuming x is not significant in comparison to h, (normal package engineering assumption)

$$d_m = \sqrt{\frac{2hW}{k}}$$

and

$$P_m = W \pm \sqrt{W^2 + 2Whk}$$

$$P_m = \sqrt{2Whk}$$

where P_m is the maximum force exerted on the mass by the spring,

and

$$G_m = \sqrt{1 + \frac{2hk}{W}}$$

$$G_m = \sqrt{\frac{2hk}{W}}$$

where G_m is the absolute value of maximum acceleration of the mass.

In the case of honeycomb cushioning material with a constant crushing stress S_A and a bearing area A, and the same assumptions as to the significance of x

$$d_m = \frac{Wh}{S_A A - W} \qquad d_m = \frac{Wh}{S_A A}$$

$$P_m = S_A A \qquad P_m = S_A A$$

$$G_m = 1 - \frac{S_A A}{W} \qquad G_m = \frac{S_A A}{W}$$

and similarly the equations can be tailored to cushioning systems with different characteristics such as cubic, tangent, or anomalous elasticity.

Returning to Figure 21 and neglecting the static displacement, it can be shown that

$$x = d_m \sin \omega t$$

and

$$\ddot{x} = -\omega \sqrt{2gh} \sin \omega t$$

where $\omega = \sqrt{k/m}$ is defined as the circular frequency and t is time.

If damping, c, is added as in Figure 22, the equation of motion upon impact becomes

$$\ddot{x} + 2\beta\omega\dot{x} + \omega^2 x = 0$$

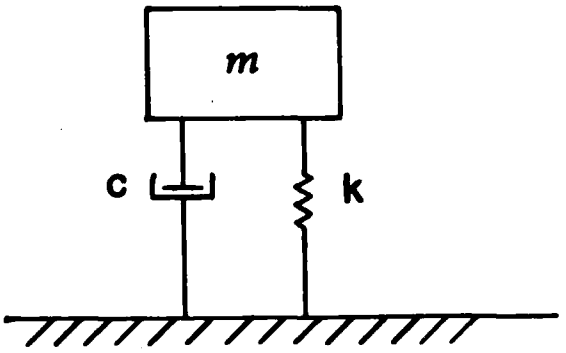

c = DAMPING COEFFICIENT

Figure 22. Damped System

where $\beta = c/2m\omega$ is the fraction of critical damping with β=0 the no-damping condition and β=1 as the no-oscillation condition. The acceleration solution for the equation of motion is

$$\ddot{x} = -\frac{\omega\sqrt{2gh}}{\sqrt{1-\beta^2}}\, e^{-\beta\omega t} \cos(\omega t \sqrt{1-\beta^2} + \gamma) \qquad (8)$$

where

$$\gamma = \arctan \frac{2\beta^2-1}{2\beta\sqrt{1-\beta^2}}$$

The effect of damping on the item acceleration is shown in Figure 23. A damped sinusoid replaces the pure sinusoid. The frequency is reduced and the initial phase is

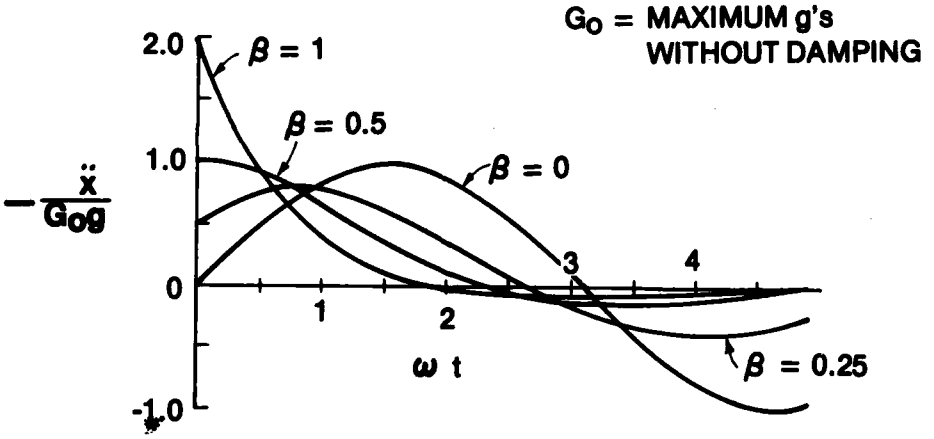

Figure 23. Acceleration-Time Curves for Linear Cushioning with Various Amounts of Damping

changed. For small damping the acceleration starts low and increases, never greater than the zero damping situation. For high damping the initial acceleration starts high and then decreases.

The effect of damping on maximum acceleration is shown in Figure 24 where,

G_m = maximum number of g's with damping

$G_o = \sqrt{\frac{2hk}{W}}$ = maximum number of g's without damping.

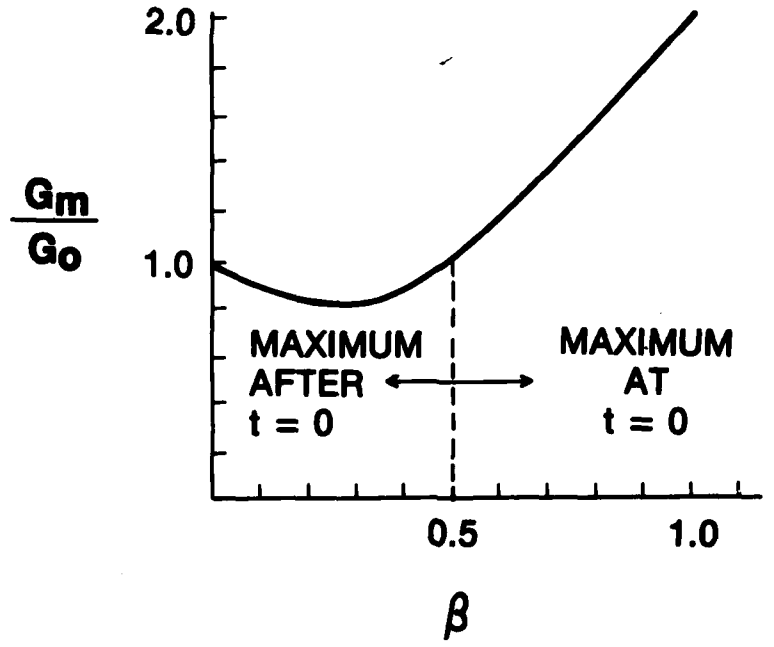

Figure 24. Effect of Velocity Damping

From equation (8) at t = 0

$$\frac{G_m}{G_o} = 2\beta \tag{9}$$

and after t = 0,

$$\frac{G_m}{G_o} = e^{-\beta\omega t_m} \tag{10}$$

where t_m, the time at which the maximum occurs, is given by

$$\tan \omega t_m \sqrt{1-\beta^2} = \frac{(1-4\beta^2)\sqrt{1-\beta^2}}{\beta(3-4\beta^2)}$$

In the figure the largest value of G_m/G_o from (9) or (10) is plotted against β. As damping is increased from zero, the maximum acceleration first decreases and then increases to

G_o at 50% of critical damping. In this interval the maximum acceleration occurs after t = 0. For damping greater than β = 0.5 the maximum acceleration occurs at the instant of contact.

The maximum acceleration experienced by the major mass of the item, however, is not always a measure of the true severity of the disturbance; as shown by Mindlin's example of a packaged item with linear undamped cushioning and perfect rebound subjected to a transient half-sine acceleration, Figure 25.

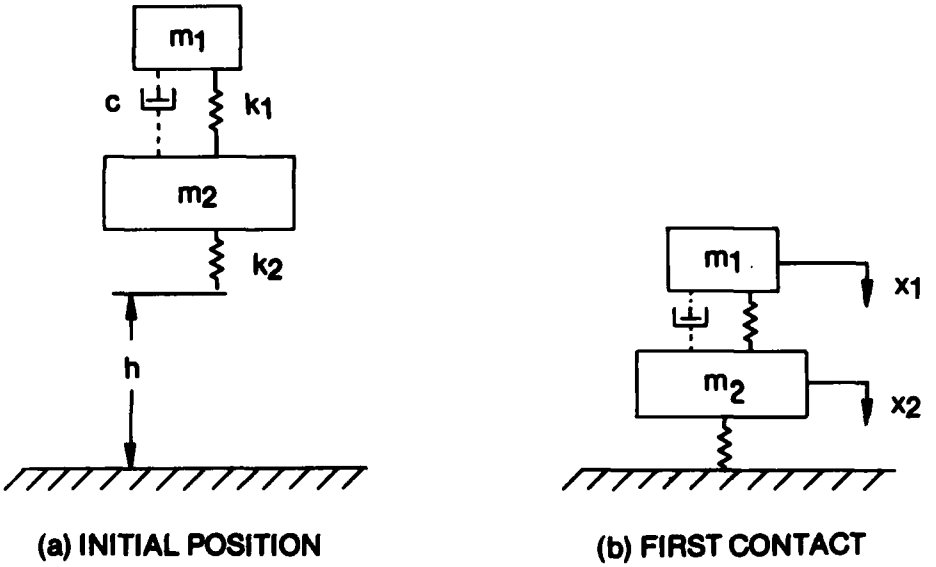

Figure 25. Idealized Linear Undamped System

If $x = x_1 - x_2$ and $m_1 \ll m_2$ and damping (c) is initially ignored it can be shown that the dynamic response is

$$x_{max} = \frac{\sqrt{2gh}}{\omega_1 (\frac{\omega_1}{\omega_2} - 1)} \sin\left[\frac{2n\pi}{\frac{\omega_1}{\omega_2} + 1}\right], \quad (0 < t < \frac{\pi}{\omega_2})$$

where n is a positive integer chosen to maximize the sine term while the argument remains less than π. The static response is

$$x_{ST} = \frac{\omega_2}{\omega_1} \sqrt{2gh}$$

and the ratio of the dynamic response to the static response, defined as the amplification factor A_m is,

$$A_m = \frac{x_{max}}{x_{ST}} = \frac{\frac{\omega_1}{\omega_2}}{\frac{\omega_1}{\omega_2} - 1} \sin\left[\frac{2n\pi}{\frac{\omega_1}{\omega_2} + 1}\right], \left(0 < t < \frac{\pi}{\omega_2}\right)$$

Similarly, after rebound, when m_1 vibrates freely with respect to m_2,

$$A_m = \frac{2\frac{\omega_1}{\omega_2}\cos\left(\frac{\pi\omega_1}{2\omega_2}\right)}{1 - \frac{\omega_1^2}{\omega_2^2}}, \quad \left(t > \frac{\pi}{\omega_2}\right)$$

Comparison of the two equations shows that when the duration of the impact is shorter than the half-period of vibration of the element the maximum displacement (and stress) in the element occurs after the impact is over.

If damping of the element m_1 is considered and expressed as a fraction (β_1) of critical damping,

$$\beta_1 = \frac{c}{2\sqrt{m_1 k_1}}$$

the amplification factor decreases as shown in Figure 26. For the curve the maximum value of A_m is 1.76 and occurs at $\omega_1/\omega_2 = 1.6$. Hence at this frequency ratio, the element deformation is 1.76 times as great as would be expected using the maximum acceleration. However, for values of $\omega_1/\omega_2 < 0.5$ the shock is less severe.

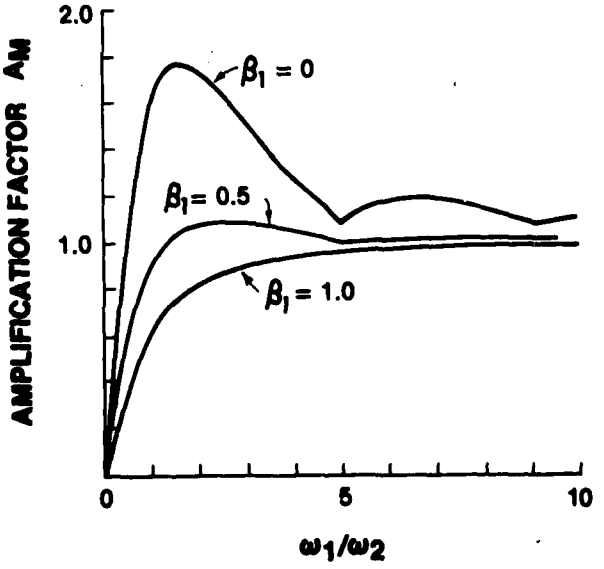

Figure 26. Amplification Factors for Linear Undamped Cushioning with Perfect Rebound

As shown, the amplification factor for a theoretical cushioning system depends on the shape of the input pulse. Some normalized examples are given in Figure 27. As can be seen from the figure, the square wave is the most damaging excitation pulse.

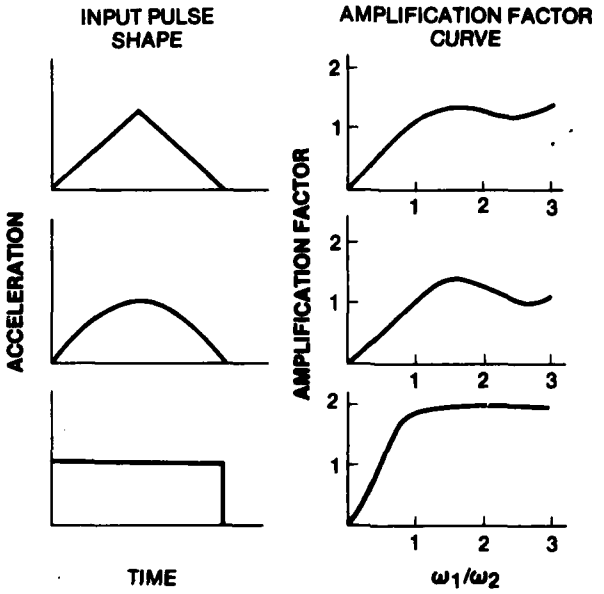

Figure 27. Normalized Shock Spectra

Fragility: The fragility (G_F) of an item is a dimensionless ratio of the maximum acceleration (a_m) that the item can withstand in any direction before breakage or malfunction due to the acceleration of gravity (g).

$$G_F = \frac{a_m}{g}$$

Essentially, the item fragility is a measure of its elasticity, the item's capability to recover its shape after the removal of a distorting force. The amplification factor, however, can produce different peak accelerations of different parts of an item as a result of a single impact; consequently, the part of the item to which the fragility rating is referred is important. Also, the fragility of the item can not be completely separated from the characteristics of the cushioning medium.

The Quartermaster Food and Container Institute for the Armed Forces conducted initial cut and try aerial delivery studies[11,24] to develop specific cushioning systems for selected resupply items, generally food, water and gasoline. These studies indicated that

[24] Roffee, B. H. Aerial Delivery System for Combat Rations with Paper Honeycomb as an Energy Absorbing Material. QMFCIAF Report, February 1956.

a more rational approach would be to determine a "damage rating" for a particular resupply item, design a cushioning system to protect to that value and then experimentally verify the system. Damage ratings for cans were determined statically with compression tests[25] and dynamically with a centrifuge.[26] Data generated was successfully used in the redesign of ration packs[27,28] to increase their strength and in the design of a high speed aerial delivery container and associated load configurations.[12,29]

These studies were expanded in cooperation with the Structural Mechanics Research Laboratory of the University of Texas to include military vehicles. Both experimental and analytical investigations were conducted to determine the resistance of the vehicles to shock and to develop appropriate cushioning systems. Honeycomb cushioning systems were developed experimentally[30] for trucks, trailers and personnel carriers.

Some pertinent results of the analytical studies are summarized:

Single-Degree-of Freedom Undamped System, Ripperger.[31]

For small values of the ratio of pulse duration to the period of the system $t/T < 0.25$, the response is determined essentially by the pulse amplitude. For values of t/T greater than 0.25 the response is determined by the pulse shape, duration and amplitude.

[25] Miller, A. Damage Susceptibility, Study of Can Damage. QMFCIAF No. 191, November 1958.

[26] Myers, E. C. The Determination of Strength of Items for Aerial Delivery Design Purposes using a Centrifuge. QMFCIAF No. 180, November 1957.

[27] Modification of C-Ration Packs for Aerial Delivery. QMFCIAF No. 190, February 1958.

[28] Venetos, M. A. Determination of Design Principles to be Employed in Development of 5/1 Ration Packs for Aerial Delivery. QMFCIAF No. 178, March 1958.

[29] Barpoulis, C. Design of Load Configurations for M–4A HSADC VI. QMFCIAF Report 4–60, March 1960.

[30] Covington, *et al.* Fragility Studies (six University of Texas reports): I, March 1960; II, April 1960; III, May 1960; IV, August 1960 (AD 246043): V, September 1960 (AD 249901); VI, July 1962 (AD 400296)

[31] Ripperger, E. A. Impact Determinations. University of Texas, October 1962 (AD 400638)

Single-Degree-of-Freedom System with Viscous Damping, Luke.[32]

Damping significantly decreases system response. Pulse shape has little effect on system response for $t/T < 0.20$. For $t/T > 0.20$ the most significant characteristic of pulse shape is rise time.

Two-Degree-of-Freedom Undamped System Subjected to Impulse Loading, Richter.[33]

For all mass ratios considered with $k_2/k_1 > 2.0$ the response is essentially the same as a one-degree-of-freedom system subjected to the same impact conditions. For $t_1/T_1 < 0.3$, where T_1 is the lower of the two coupled natural periods of the system, pulse shape has little effect on system response. For $t_1/T_1 > 0.3$ pulse rise time is the most significant characteristic of pulse shape.

Undamped Non-Linear Single-Degree-of-Freedom System Subjected to Impulse Loading, Fowler.[34]

The shape of the acceleration time pulse has a marked effect on the permanent deformation. The two parameters AT_d^2/ℓ the nondimensional displacement in a time equivalent to the natural period and TD/τ the nondimensional pulse duration seem to be the most significant in determining the deformation a given pulse will produce in a given system.

Effects of Acceleration Pulse Parameters on the Permenent Deformation of a Damped Single-Degree-of-Freedom System, Reifel.[35]

[32] Luke, R. R. The Impact Response of a Single Degree of Freedom System with Viscous Damping. June 1960 (AD 246942)

[33] Richter, A. P. The Response of a Two Degree of Freedom Undamped System Subjected to Impulsive Loading. August 1960 (AD 246944)

[34] Fowler, W. T. An Analytical Study of an Undamped Nonlinear Single Degree of Freedom System Subjected to Impulsive Loading. January 1962 (AD 276690)

[35] Reifel, M. D. The Effects of Acceleration Pulse Parameters on the Permanent Deformation of a Damped Single-Degree-of-Freedom System. January 1962 (AD 774646)

For a nonlinear yielding system, permanent deformation cannot be represented as an independent function of any one pulse parameter. For a nonlinear yielding system with constant damping subjected to a rectangular pulse of infinitesimal duration, the amplitude must approach infinity to cause any permanent deformation.

Effect of Airdrop on Complex Structures, Jan and Ripperger.[36]

The effect which small masses have on the motion of the larger masses in the system is insignificant indicating that the models of prototype vehicles can be quite simple and still give an adequate indication of the movement of the different parts during an impact.

Impact on Complex Mechanical Structures, Jan.[37]

Structural damping dissipates a considerable amount of energy, and as a consequence decreases the displacements. However, the peak accelerations at various points in the structure are affected very little by structural damping.

The US Army Natick Laboratories also conducted experimental studies[38—43] to determine the airdrop impact capability of various vehicles, missiles and ammunition. Generally, however, the experimental programs cited did not determine a fragility rating for an airdrop item. Either the item was subjected to a simulated airdrop and sufficient cushioning was added to prevent damage or a fragility rating was assumed, a cushioning system designed, and a series of drops conducted to verify or modify the design.

[36] Jan and Ripperger. The Effect of Airdrop Impact on Complex Structures. NARADCOM 70—55—AD, December 1969 (AD 711555)

[37] Jan, S. F. Impact on Complex Mechanical Structures. NARADCOM 72—49—AD, July 1971 (AD 755841).

[38] Antkowiak, H. E. Qualitative Evaluation of the Airdrop Impact Capability of the Sterilizer, Autoclave for Special Forces. NARADCOM Technical Memo AEO 16, September 1963.

[39] Antkowiak, H. E. Airdrop Impact Capability of the Redeye Missile in Model 2 and 3 Tripak Containers. NARADCOM TR 66—13—AD, March 1966 (AD 480880).

[40] Antkowiak, H. E. Airdrop Impact Capability of the Redeye Missile Unipak Container. NARADCOM TR 69—72—AD, March 1969 (AD 853098L).

[41] Antkowiak, H. E. Airdrop Impact Capability of the Redeye Missile Monopak Container. NARADCOM TR 70—53—AD, February 1970 (AD 872201L).

[42] Macek, P. A Study of the Feasibility of Airdropping Selected Ammunition without Wooden Overpacks. NARADCOM Tech Memo AEO—15, December 1963.

[43] Maschi, A. P. Airdrop Impact Capability of the Shillelagh Missile Container. NARADCOM 64—4, July 1964 (AD 455971).

The damage boundary method[44] of experimentally determining fragility ratings has been gaining acceptance recently. This concept, a product of the efforts of Michigan State University and the Monterey Research Laboratory,[45] considers the effect of peak acceleration, pulse waveform, pulse duration and velocity change on the item. The item is subjected to a series of rectangular shock pulses with various amplitudes and velocity changes on a programmable shock machine. The damage boundary for a particular item, Figure 28. is then determined by the critical velocity change line and critical acceleration line which are developed. Theoretically, if the value of velocity change the item undergoes

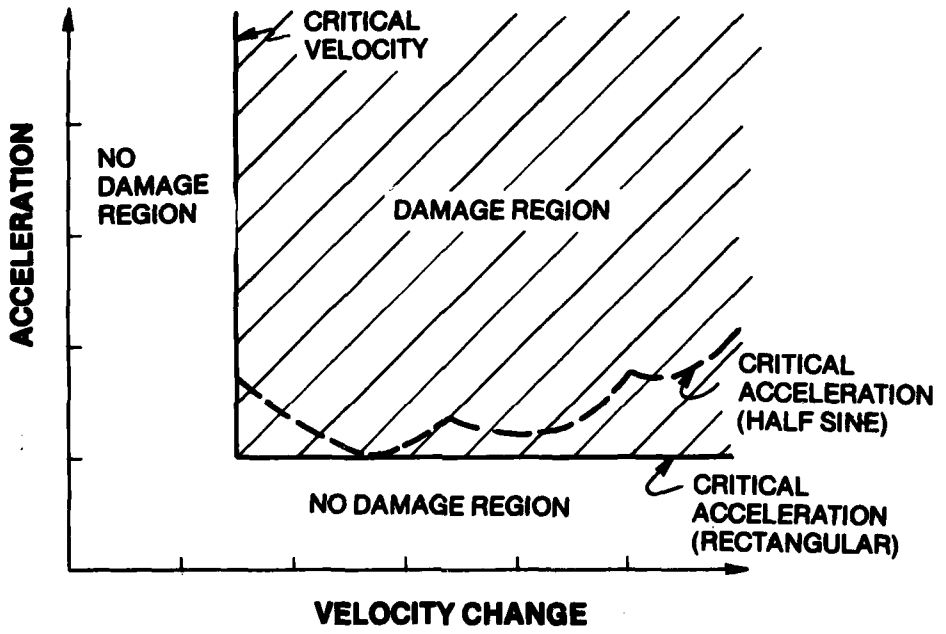

Figure 28. Damage Boundary Concept

is below the critical value no damage will result and no cushioning is required regardless of the acceleration sustained. If the value of the acceleration the item undergoes is below the critical value, no damage will result regardless of the velocity change sustained. If both the critical velocity change value and the critical acceleration value are exceeded, damage will result. The item is then protected by applying a cushioning system which

[44]ASTM D3332. Mechanical – Shock Fagility of Products, using Shock Machines. American Society for Testing and Materials. 1974.

[45]Newton, R. E. Fragility Assessment – Theory and Test Procedure. US Naval Postgraduate School, Monterey, California.

transmits no more than the critical acceleration. Reference 46 is an example of use of the damage boundary concept in determination of fragility values for an inertial guidance platform and associated gyroscope.

Fragility Testing Equipment

The impact or shock tester is the basic piece of laboratory equipment used to experimentally determine fragility ratings. The item to be tested is affixed to a moveable platen on the shock tester. The platen is then allowed to move vertically and collide at a predetermined velocity against an impact surface of known deceleration characteristics subjecting the item to a controlled impact under laboratory conditions. It has excellent repeatability. Results of tests conducted by different operators in different time periods can be compared to verify changes caused by item redesign. The shock input is programmable. Both the impact velocity and type of shock; normally half sine, sawtooth, or squarewave, can be accurately selected. The input is also controllable. Because the specimen can be attached to the drop table, it can be subjected to a single shock or shocks in different axes without the bouncing or tumbling that may occur in free fall tests.

The readout instrumentation is the same as normally required in impact testing. Accelerometers are used to measure pulse amplitude and duration. Velocity sensors are used to measure impact and rebound velocity. The sensor traces can be recorded with an oscillograph or storage oscilloscope.

Two types of shock testers, free fall and accelerated, are commercially available. The required impact velocity is obtained with the free fall tester by raising the specimen, mounted on the moveable platen, to the correct height and then releasing the platen to free fall against an elastomer or pneumatic impact surface. The accelerated impact tester is used to obtain velocities greater than can be generated in the free fall operation. The accelerated tester uses elastic cords mounted to the drop frame and table or pneumatic pressure to propel the specimen against the impact surface.

Both types of machines are limited by the maximum allowable table force. That is the maximum force generated by the impact which can be dissipated in the tester without structural damage to the machine. The table force is a function of the mass of the specimen and the impact deceleration. Generally the free fall tester has the capability of handling greater loads but at a lesser impact velocity than the accelerated shock tester. Standard shock test machines are available from the Testing Products Division of MTS Systems Corporation and/or the Electronics Division of Avco Corporation which are capable of handling specimens as great as 900 kg with projected impact areas of 152 cm x 152 cm

[46] Venetos, M. A. Determination of Fragility Values for the LN–12 Inertial Guidance Platform and Associated G–200 Gyroscope. Air Force Packaging Evaluation Agency Report 73–55, October 1973 (AD 769908)

and unlimited specimen heights. Maximum impact velocities range from 7 metres/sec to 17 metres/sec, depending on the specimen mass and impact machine. Impact decelerations of 600 g's can be attained with the large machines. Non-standard machines can be manufactured with greater capabilities.

NARADCOM has an Avco SM–020 vertical free fall drop tester which has been used primarily for package handling studies. The tester will accommodate a 60-cm-wide by 60-cm-long, 136-kg specimen directly on the platen. Longer specimens which overhang the platen can be tested if adequate support of the overhanding weight is provided. The impact velocity of this tester is limited by the height of the machine and the height of the specimen. The maximum theoretical impact velocity obtainable is 6.5 metres/sec because the maximum free fall distance is 2.3 metres. But when a fragility specimen is mounted on the platen, the maximum free fall distance is decreased by the height of the specimen and consequently the available terminal velocity is also decreased.

The machine is presently equipped with lead and elastomer pads which produce sawtooth and half sine waveforms. The maximum deceleration is 500 g's and maximum pulse duration is 20 msec but both maxima cannot be obtained simultaneously. Additional impact pads are available from the manufacturer which produce a square impact pulse.

Sled-type crash simulation systems have been used for dynamic testing of automotive components and safety devices. In the sled crash simulation system the specimen is mounted on a sled which is accelerated in the horizontal direction along a set of tracks by elastic shock cords or gas pressure and guided to collide against a stationary programmable impact surface.

The sled crash simulation systems generally are capable of impacting larger masses at greater velocity changes, e.g., 27 metres/sec, than the vertical shock testers. They have the disadvantages, however, of being much larger, 10 to 15 metres in length, more expensive, and by the nature of the instrument the impact deceleration is in the horizontal direction and not the vertical direction which would be more analogous to the aerial delivery situation.

NARADCOM has a horizontal compressive impact testing machine somewhat similar to the sled-type crash simulators. The machine was designed especially to evaluate dissipating material specimens 40 cm x 46 cm in area and up to 38 cm thick at a maximum relative impact velocity of 15 metres/sec and a maximum energy level of 16,000 joules. Because the velocity, deceleration, and carriage mass can be varied, the machine can be used for limited fragility determinations also. The compressive impact tester consists of two balanced carriages situated at opposite ends of a 12-metre track. The specimen to be tested, normally cushioning material, is affixed to one of the carriages. The carriages are propelled horizontally toward a collision at the center of the track by the action of two coordinated pneumatic cylinders. Energy input to the system is controlled from a central control panel by regulating gas pressure in the pneumatic actuators, and impact velocity is controlled by adding or removing cast iron weights to adjust the mass of the

moving carriages. Instrumentation includes an accelerometer which senses the acceleration of one carriage during impact and an electromagnetic velocity measuring system which measures relative velocities of the two carriages before, during, and after deformation of the test specimen. Outputs of the accelerometer and velocity measuring system are displayed on a dual-beam oscilloscope and recorded photographically.

The horizontal compressive impact tester can be utilized for limited fragility determinations by mounting the fragility specimen on one of the carriages and mounting a cushioning medium on the other carriage. Used in this manner the impact tester has the desirable feature of high speed impact; but because it is intended primarily for cushioning evaluation, the fragility specimen geometry and mass are limited by the method of attachment to the carriage and the shock waveform is limited to that obtainable from commercial cushioning material.

Although limited fragility determinations are possible with the compressive and free fall testers available at NARADCOM a serious program would require a different tester. One of the larger commercial programmable free fall testers previously mentioned should suffice for free drop fragility determinations because a practical free drop load would be less than the 900-kg mass and 152-cm square surface that the larger testers accommodate.

The distinction between fragility rating determination and free drop impact simulation must be kept in mind at this point. To determine an item fragility rating, the expected free drop impact velocity need not be duplicated. Only the critical velocity, a much lower value, must be attained. Therefore, comparatively low impact velocities may be used for experimental fragility determination. Impact simulation, on the other hand, however, requires that the impact velocity be duplicated. With this in mind, it is possible to determine fragility ratings in the laboratory but it is unrealistic to try to develop a practical laboratory machine to simulate free drop impact of heavy items because of the high velocity and large kinetic energy involved. Retarded airdrop impact which occurs at lower velocities, however, could be duplicated in the laboratory for many supply loads with a modified or non-standard commercial tester capable of a load of approximately 2,000 kg and an impact velocity of approximately 10 metres/sec.

Directions for Future Study

It is generally agreed that a universal solution which predicts the maximum acceleration, the form of the acceleration-time relationship, and the effect of the acceleration on the payload is not presently practical. The state of the art is equipped to estimate the peak shock developed at the interface between cushion and cushioned object, but not how elements of the cushioned object respond to peak shock and the

associated waveform.[47] At present, there is no suitable analytical[48] or generally accepted experimental technique[49] to determine the fragility of an item. This is a result of the complex failure mechanism involved when an item is subjected to different shock pulses. The maximum acceleration, the impact duration, the rise time to peak amplitude, and the natural frequency of the item have all been shown to have some influence on the damage susceptibility.

A practical approach, as depicted in Figure 29, for free drop aerial delivery, however, would be to:

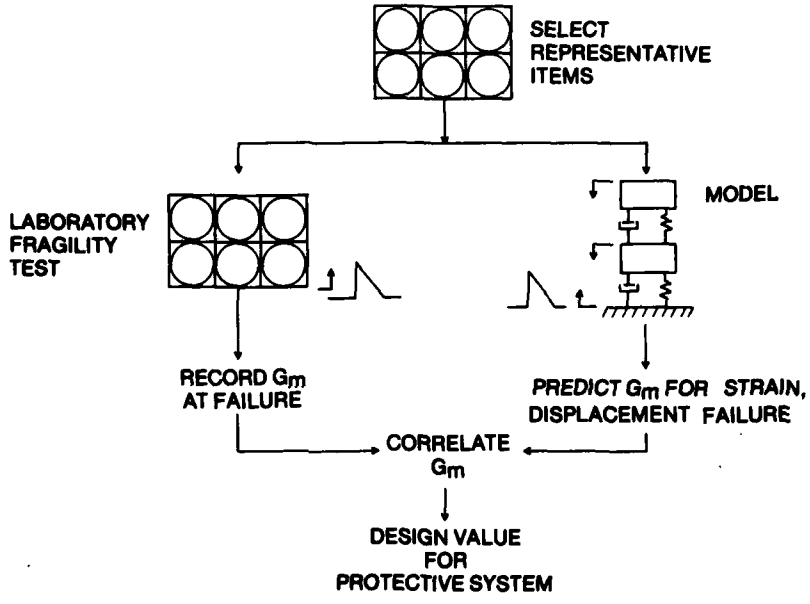

Figure 29. Determination of Fragility Design Value

Select several payloads representative of common resupply items (food, ammunition, medical supplies) and analytically model them. These items are simpler than the vehicles which have been concentrated on, thus making this task somewhat easier.

[47] Mustin, G. The Theory and Practice of Cushion Design. Shock Vibration Information Center, 1968.

[48] US Army Rocket and Missile Container Engineering Guide. Redstone Arsenal. June 1971.

[49] Package Cushioning Design. Military Standardization Handbook 304A, September 1974.

Analytically determine the response of the payloads to selected shock inputs.

Analytically determine the maximum response which the payload can withstand without damage due to strain and/or collision as a result of displacements when subjected to the selected shock inputs.

Experimentally verify the analytical models.

Use the data and models developed to determine the allowable conditions (altitude, speed, cushioning type, thickness) for successful free drop.

SHOCK MITIGATING METHODS AND PACKAGING

State of the Art

The impact deceleration shock experienced by the payload is normally decreased by use of shock mitigating systems which absorb a portion of the impact energy. Many types of shock mitigating methods have been experimented with in the past. The British used air bags as far back as 1943 to cushion a Jeep parachuted from a Halifax bomber.[50] Cellulose wadding was a standard quartermaster issue cushioning material in 1951. Crash pads filled with hemp, horsehair or felt were also common. Numerous other candidate materials and devices such as popcorn, tin cans, cellular aluminum, burlap and plastic bags, frangible tubing and a large variety of foams have been tried with various degrees of success. The standard airdrop cushioning material now in common use is paper honeycomb. It is a one-shot energy dissipator with close to the ideal rectangular energy dissipation profile.

Although it is understood that shock mitigration methods are very important, the subject is only mentioned here because it is an active well documented area[47,49,51-58]

[50] Peifer, W. H. Supply by Sky. Quartermaster Historical Studies Series II, No. 2, 1957.

[51] Baker and Mallow. Silicate Foam for Airdrop Cushioning. NARADCOM TR 68–46–AD, May 1968 (AD 669666).

[52] Fuka, L. R. Buckling of Cylindrical Shells Subjected to Axial Loading. NARADCOM TR 72–50–AD, September 1971.

[53] Hasslacker, G. J. Dynamic Properties of Energy Absorbers for Use in Aerial Delivery. QMFCIAF 10–58, June 1958 (AD 219659).

[54] Hwang, C. S. Energy Dissipation with Frangible Tubing. University of Texas, February 1965.

[55] Mathews, H. E. Development of Rubber Base for the HELO Landing Zone Locator. NOLTR 70–21, June 1970 (AD 871577).

[56] Murray, G. E. Basic Concepts on the Energy Dissipation of Cushioning Material. NARADCOM CP–12, April 1958.

[57] Tomcsak, S. L. Decelerator Bag Study. Goodyear, June 1960 (AD 243159).

[58] Young, L. D. Determination of Air Delivery System for Dry Bulk Materials using the Multiple Bag Free Fall Method. Yuma Proving Ground Report E–45, November 1959 (AD 256836L).

in which the characteristics of most commercial cushioning materials have been adequately cataloged for normal use and which does not justify additional effort specifically for free drop applications. The possibility of extending the use of commercial cushioning, other than honeycomb, especially elastomers into high speed free drop impact situations, however, would require additional data on the high speed compression characteristics of the medium. Results of research in new energy absorbers should be applied to free-drop applications as they become available.

An area which does show promise of yielding meaningful results for free drop, as well as retarded airdrop, and which is not presently being investigated is the packaging or arrangement of individual items within the payload. The Quartermaster Food and Container Institute for the Armed Forces published a report[28] in 1958 which showed that the damage resistance of the 5-in-1 Ration Pack could be increased by as much as 60% by rearranging the individual items in the pack. It was found that the main factors which should be considered in the design of can packs for aerial delivery were (1) can orientation, (2) simultaneous load pickup, (3) uniform load distribution and (4) proper vertical alignment. When the items in the payload were so arranged that—the most rugged axis was subjected to impact, the various levels of the load received the impact force simultaneously, the impact force was uniformly distributed, and the major load-bearing elements were in proper vertical alignment, then the damage resistance of the payload would be increased. A similar study of present-day ration containers could also possible result in an improved package configuration with more resistance to damage from not only airdrop but also the normal military transportation environment.

Note on Standard Analytical Technique for Honeycomb Energy Dissipator Design

The standard analytical technique for honeycomb energy dissipator design is well documented.[2,59-61] The area (A) of honeycomb cushioning required to decelerate an item is first determined by:

$$A = \frac{W(G + 1)}{S_a}$$

where

W = Weight of item, pounds

G = Fragility or G loading

S_a = Average dynamic crushing stress of energy dissipator, #/ft^2 (6300 #/ft^2 – honeycomb)

[59] Loading Environment and Related Requirements for Platform Rigged Airdrop Material. MIL–STD–669B, August 1968.

[60] Ellis, et al. Design of Cushioning Systems for Air Delivery of Equipment. Contract DA19–129–QM–1383, August 1961.

[61] Gionfriddo, M. P. Design of Cushioning Systems for Airdrop. NARADCOM 67–59–AD, February 1967.

(English units are used in this note to facilitate comparison with previously published literature.)

The necessary thickness (T) of cushioning material to prevent bottoming is then determined by

$$T = \frac{V^2}{2gGE}$$

where

V = Impact velocity, ft/sec

g = Acceleration due to gravity, 32.2 ft/sec^2

E = Design strain of cushioning material (0.7 for paper honeycomb)

Present practice dictates that the item be subjected to the maximum allowable g level. (Minimum thickness.)

An alternative approach is to subject the item to the minimum possible g loading, maximum thickness, with two contraints.

The bearing area must be large enough to support the static load.

Column buckling, instability and aircraft space, all very important parameters, must be considered.

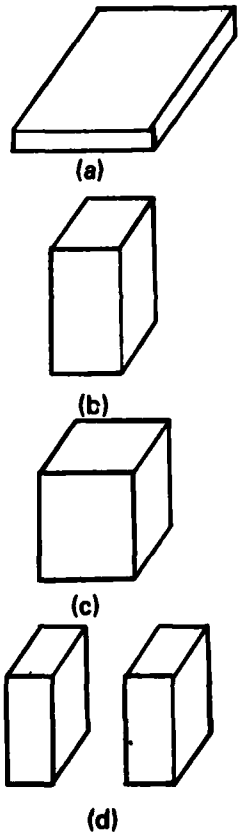

Figure 30. Honeycomb Configuration

Following this approach the maximum allowable cushioning thickness is first selected. The resulting G loading is then calculated from

$$G = \frac{V^2}{2gTE}$$

The required cushion area is then calculated from

$$A = \frac{W(G + 1)}{S_a}$$

Solutions to these equations for various impact velocities and payload weights are presented in Figure 31.

As an example of use of the two approaches, assume an item with a weight of 2000 pounds and a fragility of 50 is to impact at 28.5 ft/sec.

Following the standard technique, the item would require a honeycomb area of

$$A = \frac{W(G + 1)}{S_a}$$

$$= \frac{2000\ (50 + 1)}{6300}$$

$$A = 16.2\ ft^2$$

and a thickness of

$$T = \frac{V^2}{2gGE}$$

$$= \frac{(28.5)^2}{2(32.2)(50)(0.7)}$$

$$T = 0.36\ ft = 4.3\ inches$$

This configuration theoretically assures that the item will be subjected to the maximum allowable g loading, 50 g's, and this specific volume, 5.84 ft^3 (16.2 ft^2 x 0.36 ft) assures that the honeycomb will be able to absorb the impact energy without bottoming out.

By the alternative approach; assume aircraft space requirements limit the height of the cushioning stack to 18 inches. From Figure 31(a) for 18 inches of honeycomb and an impact velocity of 28.5 ft/sec the resulting G loading is 12 g's. And from Figure 31(b) for 12 g's and 2000 pounds the required cushion area is 4.1 ft^2. This configuration

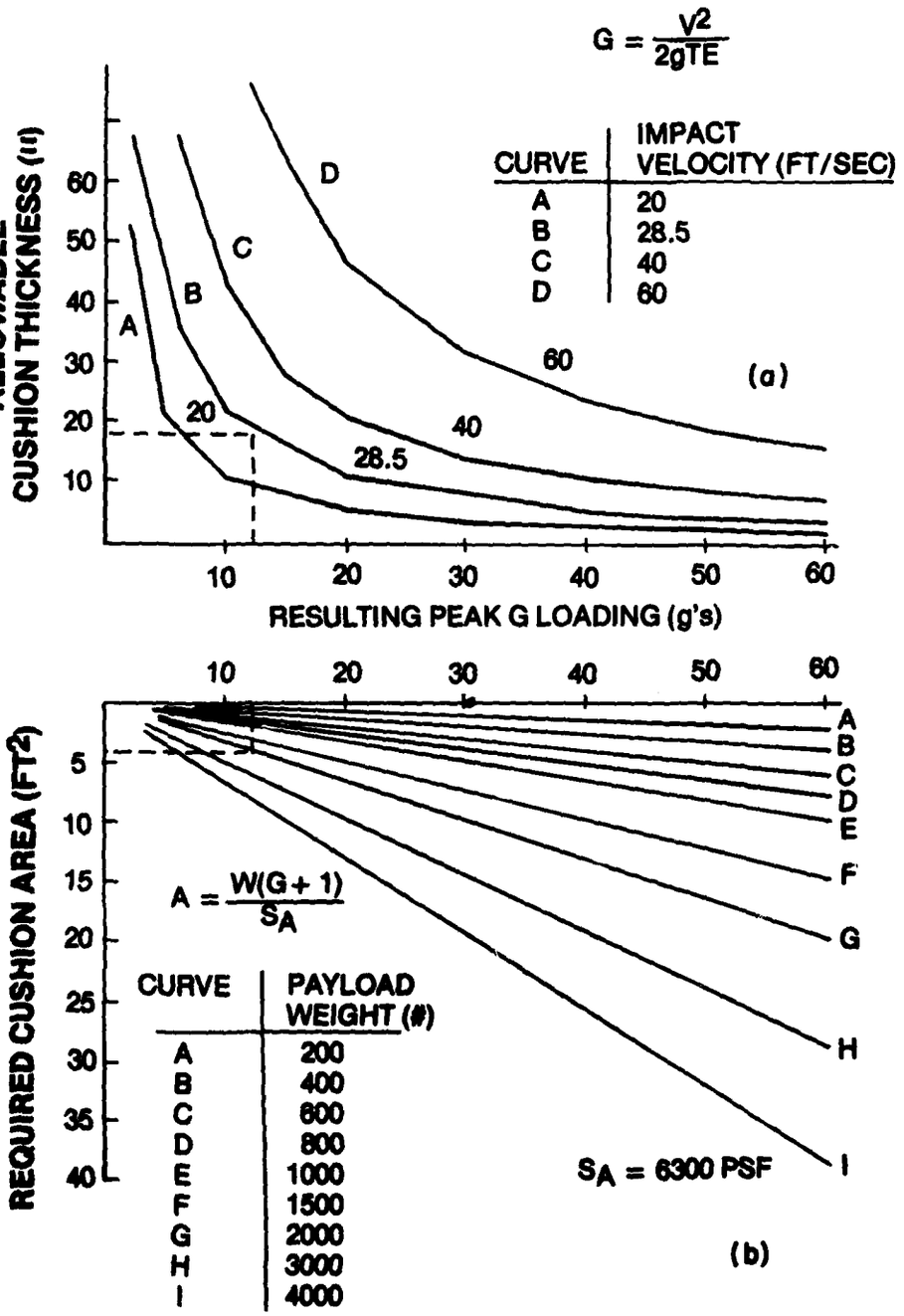

Figure 31. Cushion Area and Thickness vs G Loading

which requires slightly more honeycomb (6.15 ft^3) subjects the payload to only 12 g's, a significant increase in impact protection.

Basically, as shown in Figure 32, for areas of practical concern (above 10 g's) a specific volume of honeycomb is required to absorb the impact energy associated with the impact of a known mass at a specified velocity.

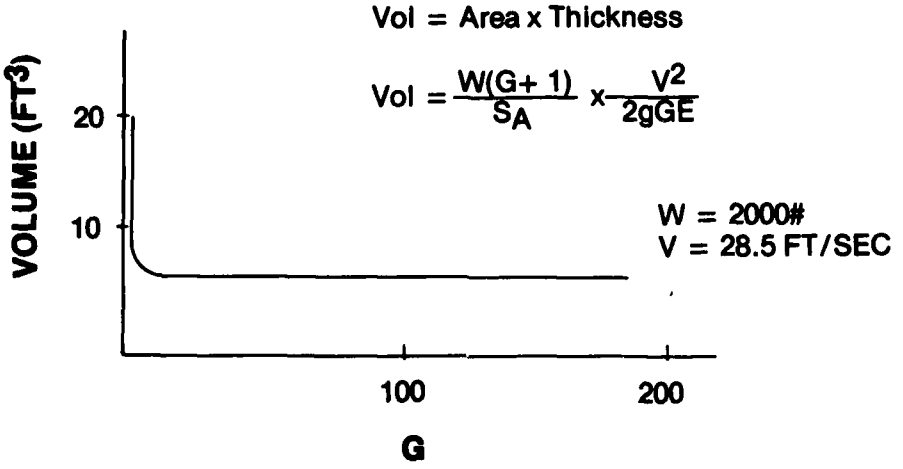

Figure 32. Cushion Volume vs G Loading

The configuration of the volume, however, determines the g level experienced by the item. As the thickness increases the g loading decreases. Therefore, the suggested approach is to design to maximum practical thickness, thereby assuring minimum practical g loading, instead of designing to minimum possible thickness which assures maximum safe g loading.

CONCLUDING REMARKS

The subjects of free fall dynamics and aerodynamics, impact dynamics and fragility, and shock mitigating methods and packaging have been addressed to determine the present state of the art in the design of free drop aerial delivery systems. The basic interrelationships among the critical areas which must be addressed in the design of free drop systems are:

(1) Free fall dynamics result in initial ground contact with a certain attitude and amount of kinetic energy.

(2) The cushioning system configuration and properties must accommodate the attitude and quantity of kinetic energy produced during the free fall and then must generate an input pulse with a duration and shape which are amenable with the fragility properties of the actual item in its common packaging.

These relationships can be diagrammed as in Figure 33.

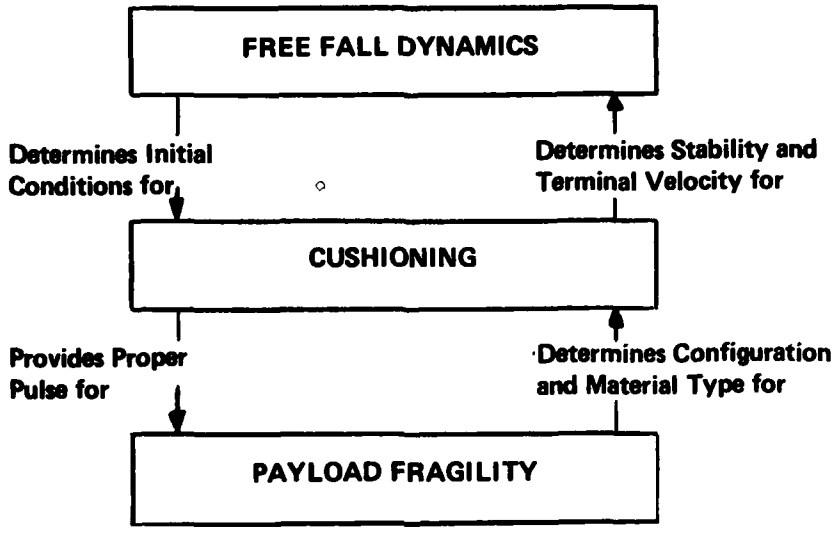

Figure 33. Basic Relationships

The survey shows that all areas lack some data for the rational design of free drop systems. The design of packaging systems for specific Army payloads will require:

(1) The determination of the fragility of the item(s) and of the preferred impact attitude and/or the preferred arrangement of items within the payload to provide the maximum fragility rating;

(2) The deign of an outermost container with selectable cushioning characteristics which will also allow for impact in a given attitude.

In addition, if maximum accuracy of delivery is to be achieved, studies are needed to generate drag coefficients for common payloads, develop data on the characteristics of delivery aircraft which affect trajectory prediction and to develop aircraft release techniques which will minimize drop release time and thus the resultant scatter on the drop zone.

Scenarios for future conflicts predict the wide dispersion of combat units on the battlefield. If resupply by aerial delivery is contemplated, then free drop systems may have particular application since they are most effective for small supply units and appear capable of effective use for food, water, clothing, some munitions, medical supplies, decontamination supplies and maintenance items. In the past, free drop systems have been developed by a cut-and-try technique as needed with varied degrees of success. In future conflicts time for such on-the-spot developments may not be available. If combat planners anticipate the need for such resupply in future conflicts of small combat units widely dispersed on the battlefield then specific payloads of potential need should be identified and the technology base developed for the free drop of these payloads in a highly accurate and successful manner so that the detailed packaging instructions and material will be available when needed.

REFERENCES

1. STREETER, V. L. Determination of Momentum of Air Dropped Shipping Containers. (Two ITT reports), November 1949 (AD 473134); March 1950 (AD 473135).

2. Design for Air Transport and Airdrop of Materiel - Engineering Design Handbook. AMCP 706-130, December 1967.

3. Low Altitude Air Drop System. ER 3980. Aircraft Armaments, Inc., May 1965.

4. TURNACLIFF and HARTNETT. Generalized Trajectories for Free-Falling Bodies of High Drag. WADC, August 1957 (AD 142300).

5. DEHMER, P. A. Free Fall Delivery, C-119 Aircraft. TAC Test 68-208, June 1969 (AD 864073).

6. Computed Air Release Systems Procedures. TACM 55-40, November 1971.

7. HOERNER, S. F. Fluid Dynamic Drag. Hoerner Fluid Dynamics. 1965.

8. BARNARD, G. et al. Development of a High Level Container Airdrop System. AIAA Paper No. 75-1386, November 1975.

9. ILVES and FIORENTIO. Free Drop Test of Thai Combat Ration. July 1967 (AD 822885).

10. Development of 25-Gallon Free Drop Aerial Delivery Fuel Containers. US Rubber Co., December 1958.

11. HEICK, R. J. Dynamic Energy Absorbing Characteristics of Paper Honeycomb Determined by Airdrops. (Five QMFCIAF reports): No. 70, April 1955 (AD 73431); No. 74, May 1955 (AD 73432); No. 98, October 1955; No. 99, October 1955; No. 108, December 1955.

12. VENETOS, M. A. Design of Load Configurations for the M-4 High Speed Aerial Delivery Container. (Eight QMFCIAF reports): No. 14-59, May 1959; No. 22-59, June 1959; No. 203, July 1959; No. 28-59, October 1959; No. 3-60, February 1960; No. 217, June 1960; No. 19-60, July 1960; No. 4-61, March 1961.

13. WILLIAMS, E. F. Research on Experimental High Velocity Airdrop Systems. QMFCIAF No. 170, February 1956.

14. Investigation of Stored Energy Rotors for Recovery, WPAFB ASD-TDR-63-745, December 1963.

15. Container, Free Drop, Map and Photo. Republic Aviation Corp., September 1960.

16. McCOLLOUGH, R. B. The Construction of a Toroidal Deceleration/Flotation Device. AFSWC-TR-73-44, December 1973 (AD 915754L).

17. PENN, J. Feasibility Study of Rotochute Decelerator for Tactical Weather Buoy. Naval Avionics Facility TR-1015, April 1976 (AD 891605L).

18. WHITE, G. B. A Design Analysis of Directional Control Systems Applicable to Air Dropped Packaging. Midwest Research Inst Report, February 1956.

19. BURT, T. E. Engineer Design Test of Meal, Ready to Eat, Individual. May 1964 (AD 847785).

20. DOMMASCH, et al. Airplane Aerodynamics. Third Edition. Pitman Aeronautical Publications, 1961.

21. PETRY, G. A. Airdrop Error Analysis, WPAFB, June 1975 (ADA 020282).

22. FARINACCI and BRUNER. High Level Container Airdrop System. NARADCOM 73-55-AD, March 1973.

23. MINDLIN, R. D. Dynamics of Package Cushioning. Bell Telephone Systems Technical Publications Monograph B-1369, 1945.

24. ROFFEE, B. H. Aerial Delivery System for Combat Rations with Paper Honeycomb as an Energy Absorbing Material. QMFCIAF Report, February 1956.

25. MILLER, A. Damage Susceptibility, Study of Can Damage. QMFCIAF No. 191, November 1958.

26. MYERS, E. C. The Determination of Strength of Items for Aerial Delivery Design Purposes using a Centrifuge. QMFCIAF No. 180, November 1957.

27. Modification of C-Ration Packs for Aerial Delivery. QMFCIAF No. 190, February 1958.

28. VENETOS, M. A. Determination of Design Principles to be Employed in Development of 5/1 Ration Packs for Aerial Delivery. QMFCIAF No. 178, March 1958.

29. BARPOULIS, C. Design of Load Configurations for M-4A HSADC VI. QMFCIAF Report 4-60, March 1960.

30. COVINGTON, et al. Fragility Studies (six University of Texas reports): I, March 1960; II, April 1960; III, May 1960; IV, August 1960 (AD 246043); V, September 1960 (AD 249901); VI, July 1962 (AD 440296).

31. RIPPERGER, E. A. Impact Determinations. University of Texas, October 1962 (AD 400638).

32. LUKE, R. R. The impact Response of a Single Degree of Freedom System with Viscous Damping. June 1960 (AD 246942).

33. RICHTER, A. P. The Response of a Two Degree of Freedom Undamped System Subjected to Impulsive Loading. August 1960 (AD 246944).

34. FOWLER, W. T. An Analytical Study of an Undamped Nonlinear Single Degree of Freedom System Subjected to Impulsive Loading. January 1962 (AD 276690).

35. REIFEL, M. D. The Effects of Acceleration Pulse Parameters on the Permanent Deformation of a Damped Single-Degree-of-Freedom System. January 1962 (AD 774646).

36. JAN and RIPPERGER. The Effect of Airdrop Impact on Complex Structures. NARADCOM 70-55-AD, December 1969 (AD 711555).

37. JAN, S. F. Impact on Complex Mechanical Structures. NARADCOM 72-49-AD, July 1971 (AD 755841).

38. ANTKOWIAK, H. E. Qualitative Evaluation of the Airdrop Impact Capability of the Sterilizer, Autoclave for Special Forces. NARADCOM Technical Memo AEO 16, September 1963.

39. _____ Airdrop Impact Capability of the Redeye Missile in Model 2 and 3 Tripak Containers. NARADCOM TR 66-13-AD, March 1966 (AD 480880).

40. ANTKOWIAK, H. E. Airdrop Impact Capability of the Redeye Missile Unipak Container. NARADCOM TR 69-72-AD, March 1969 (AD 853098L).

41. _____ Airdrop Impact Capability of the Redeye Missile Monopak Container. NARADCOM TR 70-53-AD, February 1970 (AD 872201L).

42. MACEK, P. A Study of the Feasibility of Airdropping Selected Ammunition without Wooden Overpacks. NARADCOM Tech Memo AEO-15, December 1963.

43. MASCHI, A. P. Airdrop Impact Capability of the Shillelagh Missile Container. NARADCOM 64-4, July 1964 (AD 455971).

44. ASTM D3332. Mechanical-Shock Fragility of Products, using Shock Machines. American Society for Testing and Materials. 1974.

45. NEWTON, R. E. Fragility Assessment - Theory and Test Procedure. US Naval Postgraduate School, Monterey, California.

46. VENETOS, M. A. Determination of Fragility Values for the LN-12 Inertial Guidance Platform and Associated G-200 Gyroscope. Air Force Packaging Evaluation Agency Report 73-55, October 1973 (AD 769908).

47. MUSTIN, G. The Theory and Practice of Cushion Design. Shock Vibration Information Center, 1968.

48. US Army Rocket and Missile Container Engineering Guide. Redstone Arsenal. June 1971.

49. Package Cushioning Design. Military Standardization Handbook 304A, September 1974.

50. PEIFER, W. H. Supply by Sky. Quartermaster Historical Studies Series II No. 2, 1957.

51. BAKER and MALLOW. Silicate Foam for Airdrop Cushioning. NARADCOM TR 68-46-AD, May 1968 (AD 669666).

52. FUKA, L. R. Buckling of Cylindrical Shells Subjected to Axial Loading. NARADCOM 72-50-AD, September 1971.

53. HASSLFACKER, G. J. Dynamic Properties of Energy Absorbers for Use in Aerial Delivery. QMFCIAF 10-58, June 1958 (AD 219659).

54. HWANG, C. S. Energy Dissipation with Frangible Tubing. University of Texas, February 1965.

55. MATHEWS, H. E. Development of Rubber Base for the HELO Landing Zone Locator. NOLTR 70-21, June 1970 (AD 871577).

56. MURRAY, G. E. Basic Concepts on the Energy Dissipation of Cushioning Material. NARADCOM CP-12, April 1958.

57. TOMCSAK, S. L. Decelerator Bag Study. Goodyear, June 1960 (AD 243159).

58. YOUNG, L. D. Determination of Air Delivery System for Dry Bulk Materials using the Multiple Bag Free Fall Method. Yuma Proving Ground Report E-45, November 1959 (AD 256836L).

59. Loading Environment and Related Requirements for Platform Rigged Airdrop Material. MIL-STD-669B, August 1968.

60. ELLIS, et al. Design of Cushioning Systems for Air Delivery of Equipment. Contract DA19-129-QM-1383, August 1961.

61. GIONFRIDDO, M. P. Design of Cushioning Systems for Airdrop. NARADCOM 67-59-AD, February 1967.

BIBLIOGRAPHY

ANONYMOUS. Airdrop Capability of Material. TECOM Test Procedure 7-2-509, February 1972 (AD 740655).

_____. Laboratory Evaluation Report of Free Drop Containers for Liquids. NARADCOM Interim Report, March 1966.

_____. Report on Free-Fall Door Load Bundles. Joint Air Transport Establishment. November 1972 (AD 907661).

_____. Screw Worm Fly Eradication Support. Eglin AFB, SAWC-TDR-67-1-J-1, April 1968 (831571).

BARNICLE, E. J. Military Potential Test of Interim High Level Container Air Drop System. NARADCOM TR 74-23-AD, November 1973.

BOOKER and JONES. A Kinetic-Energy Penetrator for the Deployment of Instrumentation Below Sea Ice. Defense Research Establishment Report TN-2079/74, March 1974 (AD 919990).

BRENNAN, J. N. Bibliography on Shock and Shock Excited Vibrations. Penn State University. Contract DA19-129-QM-804. August 1958.

BROWNING, A. C. A Theoretical Approach to Air Bag Shock Absorber Design. February 1963 (AD 421946).

BURT, T. E. Engineer Design Test of "M" Packet. February 1965 (AD 864073).

CARR, R. I., et al. The Effects of Shape of Load Pulse on Shock Mitigating Characteristics of a Styrofoam Plastic. July 1965 (AD 623317).

DALE and LUDWIG. Foamed Sulphur for Airdrop Cushioning. NARADCOM 68-67-AD, May 1968 (AD 673146).

FIRTH and REICHHOLD. Noncommunication Expendable Jammer Investigations. April 1964 (AD 443097).

FISHER, L. J. Landing - Impact - Dissipation Systems. NASA Tech Note D-975, December 1961.

GIONFRIDDO, M. P. Qualitative Evaluation of the Airdrop Impact Capability of the M44 Incapacitating Cluster. NARADCOM Tech Memo AEO-14, October 1963 (AD 438014).

HARMON, R. C. Development Test II of Meal, Ready to Eat, Individual. May 1974 (AD 921363).

HEICK, et al. Research on Experimental High Velocity Aerial Delivery Systems. (Ten QMFCIAF reports): No. 122, April 1956; No. 127, May 1956; No. 131, July 1956; No. 135, July 1956; No. 136, July 1956; No. 141, September 1956; No. 143, September 1956; No. 147, October 1956; No. 156, May 1957; No. 159, May 1957.

JUDGE, T. Evaluation of 5-Gallon Capacity Air Droppable Container. NARADCOM Tech Memo 69-1, January 1969.

KARNES, et al. High Velocity Impact Cushioning, Part V, Energy Absorbtion Characteristics of Paper Honeycomb. Contract DA19-129-QM-817, May 1959.

KLINGENBERG, A. D. The Theory and Operation of a Dynamic Tester for Evaluating Package Cushioning Material. WADC TR-56-342, September 1956 (AD 097327).

KROKOVER, S. The Theory and Operation of a Dynamic Tester for Evaluating Package Cushioning Material. WADC TR 56-342-1, May 1958 (AD 915754).

LYONS, W. J. Impact Phenomena in Textiles. NARADCOM TS-120, August 1962.

MADAFFER, M. C. Evaluation of Three Types of Airbag Decelerators by Drop Tests. December 1953 (AD 857025).

MASCHI, A. P. Energy Dissipation Characteristics of Hand Expanded Paper Honeycomb. February 1964 (AD 451107).

McGEHEE, J. R. An Expandable Gas Bag Concept for a Stowable, Omnidirectional, Multiple Impact Landing System. NASA N68-33736, March 1967.

PINKSTON, W. R. Air Delivery Engineering Study of High Velocity Parachute Delivery of Combat Rations. Yuma Proving Ground TR E-52, January 1961.

PULO, E. J. Static Compression Tests of Honeycombed Paper Board. QMFCIAF No. 24-57, August 1957.

REIFEL, M. D. An Analytical Study, Including the Effects of Rotary Inertia and Shear, of the Response of Elastic Beams Subjected to Acceleration Pulses. January 1964 (AD 441172).

RIPPERGER, E. A. Variations in the Crushing Strength of Paper Honeycomb. NARADCOM 70-57-AD, December 1969.

_____. The Crushing Strength of Paper Honeycomb. NARADCOM 73-71-AD, March 1973.

SCHEMBOR, E. H. Bibliography of Technical Reports and Articles Covering Complete Aerial Delivery Research Activities Conducted at the QMFCIAF from 1954 to 1962. QMFCIAF No. 239 (AD 400338).

WHITE, G. B., et al. Research on Experimental High Velocity Aerial Delivery Systems. (Eight QMFCIAF reports): No. 149, October 1956; No. 152, December 1956; No. 153, January 1957; No. 157, April 1957; No. 158, June 1957; No. 161, June 1957; No. 162, July 1957; No. 165, October 1957.

WIEDERANDERS, D. G. Ground Impact Shock Mitigation Drive-Off System Development, Cargo Truck, 3/4 Ton M37. NARADCOM 68-48AD, July 1967 (AD 667937).

_____. Ground Impact Shock Mitigation Cargo Trailer M101, 3/4 Ton. NARADCOM 68-51AD, July 1967 (AD 667938).

WONG, H. Evaluation of Energy Dissipating Materials for use in Aerial Delivery of C-Rations. NARADCOM PSR No. 4, July 1959.